THESIS

ION IMPLANTATION BORIDING OF α-IRON AND M2 STEEL

Submitted by

John Davis

Department of Mechanical Engineering

In partial fulfillment of the requirements

for the Degree of Master of Science

Colorado State University

Fort Collins, Colorado

Fall 1997

COLORADO STATE UNIVERSITY

September 12, 1997

WE HEREBY RECOMMEND THAT THE THESIS PREPARED UNDER OUR SUPERVISION BY JOHN DAVIS ENTITLED ION IMPLANTATION BORIDING OF α-IRON AND M2 STEEL BE ACCEPTED AS FULFILLING IN PART REQUIREMENTS FOR THE DEGREE OF MASTER OF SCIENCE.

Committee on Graduate Work

Robert E. Lee

Paul J. Wilbur

Advisor

Department Head/Director

ABSTRACT OF THESIS

ION IMPLANTATION BORIDING OF α-IRON AND M2 STEEL

Boriding, a thermochemical diffusion process, traditionally has been used to create wear resistant boride layers on the surface of metals. Traditional pack, bath and gas boriding methods use large amounts of heating power and consume large amounts of boron containing material, which in some cases can be toxic or corrosive. It is argued that boron ion implantation at elevated temperatures is an attractive alternative to conventional boriding. To avoid the problems of traditional boriding techniques boron was ion implanted at a low energy, 20 keV, into iron and M2 tool steel from a high-current-density (500 $\mu A/cm^2$), broad-beam (5 cm) ion source which uses solid boron instead of a boron-containing gas to create boron ions. Iron and M2 steel were implanted over a range of high substrate temperatures to allow the study of thermochemical diffusion beyond the ballistic depth of implantation and to facilitate the formation of iron borides.

It is shown that the Fe_2B and $Fe_{23}B_6$ are the predominant borides formed while no indication of the brittle FeB phase, which is typically formed with conventional boriding, is found. These borides are shown to be more wear resistant than untreated iron and M2 steel that has seen the same thermal cycle.

Activation energies and the pre-exponential of the Arrhenius diffusion equation for boron in iron were found to be 0.76 eV/atom and 7.0 x 10^{-8} cm^2/s, while those for M2 steel were 1.43 eV/atom and 8.93 x 10^{-5} cm^2/s.

John Davis
Department of Mechanical Engineering
Colorado State University
Fort Collins, CO 80523
Fall 1997

Acknowledgments

No project is ever done alone, so I would like to acknowledge some of the people who made this possible.

First and foremost is my advisor, Dr. Paul J. Wilbur. Without Dr. Wilbur's patience and instruction I would never have been exposed to the world of plasmas and thin films. I will never be able to repay him for the time and energy he spent making sure I did things correctly and understood why I was doing them.

Dr. Don Williamson from Colorado School of Mines and Mr. John Vajo and Dr. Ronghua Wei from Hughes Research Laboratories for their time and effort at collecting surface analysis data for me. Dr. Williamson was responsible for the X-ray diffraction and Mossbauer data, while Mr. Vajo and Dr. Wei were responsible for the Auger electron spectroscopy data in this thesis. Without their help this thesis would consist only of optical microscopy and wear test data. Truly the data they gathered for me allowed for a much better investigation.

Dr. Don Radford and Dr. Robert Lee should be acknowledged for their part in my personal and professional development. They not only played an invaluable role on my graduate committee but also imparted their knowledge to me both through their classes and in one-on-one situations.

Dr. Ikuya Kameyama, Steve Snyder, Dave Burtner and Tim Baker who made each and every day in the lab enjoyable.

Dave Olivero and Mike Huber, two of the best roommates a guy could have. They kept me sane when I needed to be sane and insane when I needed to be insane.

To Kathryn, who has become an integral part of my life. One in which I would truly miss if it didn't exist.

My mother and father, who have stood by me no matter what. Their faith in my abilities has been unwavering since the day I was born. Without their help and encouragement I would have never made it to a point where graduate school was even possible.

Finally I would like to acknowledge the National Science Foundation for Grant CMS-9414459 which funded this research.

Table of Contents

Table of Figures

1.0 Introduction

The annual cost of the waste associated with unnecessary wear and friction is tremendous. For example, a 1976 study of this waste suggested that in the United States it was as great as tens of billions of dollars per year.[1] A substantial fraction of this waste can be traced to the time and money lost when metallic parts such as cutting tools, bearings, gears, etc. wear to the point where they are no longer serviceable and must be replaced.[1,2]

One method of increasing the wear resistance of metallic components, thereby increasing their useful lifetimes, involves alteration of their surface properties. This can be done by diffusing boron into the surface using a process variously called boriding or boronizing.[3] The process is similar to the more popular carburizing and nitriding processes which of course involve diffusion of carbon and nitrogen. In all cases, however, the final objective is generally the formation of a surface layer that is saturated with hard, wear-resistant borides, carbides or nitrides. Boriding is attractive because it yields a surface that is arguably more wear-resistant than ones treated using carburizing, nitriding and various other treatments. This was shown by Budinski [4], Hunger and Trute [5], and Sinha [6] who have studied many surface treatments under a variety of wear states (e.g. adhesive and abrasive) and found that borided surfaces typically exhibit order-of-magnitude-greater wear resistances than nitrided or carburized surfaces. In addition, Erdemir, et al. [7,8], showed that a borided surface can tend to release a natural, solid lubricant which facilitates reductions in both wear and friction. This occurs because boron from the surface can react with moisture in the atmosphere to form boric acid, a substance that has a layered structure similar to that of graphite.

Borided surfaces are also attractive because they are:

- Hard. Iron borides are reported to have a hardness that is equivalent to that of tungsten carbide [6] and higher than nitrided and carburized layers.[9]
- Hard at high temperatures. Borided layers retain their hardness at higher temperatures than nitrided layers.[6]
- Very resistant to corrosion in non-oxidizing acids and alkalis.[6]
- Resistant to molten metal attack.[6]
- Moderately resistant to oxidation to 850 °C.[6]
- Heat treatable. Heat treatment of the base material can be done after the boriding process without affecting the boride layer provided the temperature remains below the eutectic point of the iron-boron system (1150 °C).[10]

Borided surfaces are relatively unattractive because they are [6]:

- Expensive. Traditional boriding is more costly than carburizing or nitriding.
- Subject to growth during processing. During boriding, surface layers expand 5 to 25% of their pre-treatment thickness, depending on the base material. For precision parts this growth must be taken into account.

Finally it is noted that boriding induces only marginal improvement in the fatigue endurance limit of a surface.

1.1 Methods of Boriding

In order to take advantage of the attractive features of borided surfaces and make them competitive with nitrided and carburized ones, it will be necessary to reduce their costs. These costs are determined mainly by the processing method and associated boron-donating medium that is selected. The conventional boriding methods that are used along with their pros and cons are:

1.1.1 Pack Boriding - This process involves the packing of a powder mixture containing a boron-donating compound, an activator, and a dilutant around the surface to be borided.[3] The pack and substrate are then raised to a temperature between 800 and 1100 °C. In this temperature range the activator, usually a fluoride or chloride compound dissociates. The halide part of the activator reacts with the boron donor, usually amorphous boron or boron carbide, to form a boron-halide gas. The boron is then transported to the surface in the gas. When the gas comes in contact with the surface, it dissociates thereby enabling boron diffusion into the surface and leaving the halide free to react with more of the boron-donor compound.[11-13]

Pros:

- This is the best understood and, therefore, most popular method for commercial applications [3,9,14,15] and research purposes.[11-13,16-28]
- No toxic gases or corrosive salt baths are involved.

Cons:

- The rates of boron delivery to a surface and distribution beneath that surface are limited by several reaction and diffusion rates that can be controlled only via a single parameter, namely the system (boron pack and component) temperature.[11]
- The high temperatures required to assure high boron delivery rates and short processing times yield brittle layers associated with both FeB and Fe_2B formation on steels.[11]
- The processing energy requirement is great because the pack, component and chamber must all be heated to the processing temperature.
- The pack contains a limited amount of boron so the available boron and its rate of delivery both decrease as the processing proceeds.
- Safe disposal of the flouride- and/or chloride-bearing pack materials is expensive.
- Pack materials, which stick to the surface during processing, must be removed using post-processing grinding.[11]

The inability to provide independent control of the temperatures of the pack and the part being borided constitutes an important limitation for pack boriding. It is a limitation because a single system temperature will generally yield a boron delivery rate to a surface that is incompatible with the diffusion rate beneath that surface. This leads to the formation of a dual-layer (FeB over Fe_2B) when iron or steel is processed. The FeB component is undesirable for wear applications because it is more brittle than Fe_2B and because the combination yields residual stresses (tensile in the FeB surface layer and compressive in the Fe_2B beneath it). The opposing stresses can cause cracking at

or near the FeB/Fe_2B interface and this will result in flaking or spalling of the FeB during wear.[6] The creation of a simple Fe_2B layer is preferred. If FeB is created during boriding it can be diffusion annealed to form Fe_2B, but this adds another step to the processing.[5] Once it forms, Fe_2B will remain stable and not dissociate or diffuse until the iron-boron eutectic temperature is reached at 1150°C. This high temperature stability enables heat treatment of most metals after the boriding process is completed, thus taking advantage of the best properties of both the boride layer and the substrate material.

Companies like Elektroschemelzwerk Kempten GmbH [3,14] in Germany and Lindberg Heat Treating Co. [9,10] in Rochester, NY have been using the pack boriding method for years and they claim reduced wear and longer product life in a number of applications. For example, stainless steel (17% Cr) perforated strips used in the tobacco industry are borided to increase their service life 25-fold. Borided grinder disks in a commercial coffee roasting plant have five times the life of untreated disks. Borided oil-pump drive gears in the Diesel engine of Volkswagen Golf vehicles performed so well that they became a standard item on this model.[14]

There is a hybrid-pack method, called Borudif [11], that involves BF_3 production and transport to a surface through a pack of B_4C/SiO_2 activator rather than traditional activators like KBF_4/BaF_2. The method is attractive because KF, which forms from KBF_4, melts at pack boriding temperatures, sticks to surfaces and is costly to remove.

1.1.2. Bath Boriding - The component is submerged in a hot bath of molten, boron-containing liquid that is usually composed of borax and other salts.[3] In some cases, the component is biased electrically and borided electrolytically.[29] Both of these processes are usually carried out above 850 °C, because the borax is too viscous to be usable below this temperature. Borax diluted with NaCl and pure borax must be raised to temperatures above 900 °C and 1000 °C, respectively to realize sufficiently low viscosities.[29] The bath process is used less than pack boriding.[3,6,27,29,30,31]

Pros:

- The bath liquid can be circulated to assure a uniform boron distribution on all surfaces.
- The components can be put directly into a hot bath. This eliminates the necessary heat up of the entire system for each part or batch, as seen with the pack boriding method.

Cons:

- The rate of boron delivery to a surface is determined by the viscosity of the salt bath and rate at which the boron-containing compound dissociates. These rate-controlling steps are both determined by a single parameter, the system temperature.
- The high temperatures required to assure a low viscosity yield boron delivery rates that result in the formation of an FeB/Fe_2B dual layer rather than a simple Fe_2B layer.[29]

- The boron supply in the bath is limited so the boron concentration and delivery rate to the surface diminish with processing time.[3]
- The processing energy requirement is great because the component, bath and container must all be heated to and held at the processing temperature.
- Disposal of the salt bath in an environmentally acceptable manner is costly.
- Most applications require that the molten salts be washed off the substrate before they are usable and this adds a post-processing step.[3,6,29]

1.1.3 Gas Boriding - The component is placed in a furnace, where it is heated either through radiation from the walls of the furnace or by conduction. Boron-containing gas is then circulated around the hot component. When the gas comes in contact with the component surface it dissociates leaving boron that can diffuse through the surface into the component. The gases that are used in this process include BCl_3, BF_3, BI_3, BBr_3 and B_2H_6.[3,32-34]

Pros:

- The gas circulates readily and this enables good surface-treatment uniformity.[3]
- Post processing to remove surface contaminants is not required.
- Treatment can be effected at temperatures as low as 700°C.[32]
- The boron-bearing gas can be renewed continuously to assure boron concentration will remain uniform in time.

Cons:

- The rates of boron delivery to the surface via decomposition of the gas and diffusion into the material are both determined by a single parameter, the system temperature.[3]
- The gases used for this process are either highly corrosive, highly reactive (especially with water vapor), highly toxic or combinations of these. Consequently, great care must be exercised to prevent damage to the processing equipment and harm to people.[3,14]

Because of concerns over boriding gases, it appears that this process has seen research attention but no commercial application scale.[32-36] If commercial application were possible, the rates of boron delivery to the surface and diffusion beneath it would still be determined by the component temperature and could, therefore, not be controlled independently.

1.1.4 Plasma Boriding - This is a modified gas-boriding process in which a boron-plasma glow discharge is established between a cathode-potential component and an anode which may be either the chamber walls or a separate plate.[37-40] The gases, which are the same as those used for gas boriding, are dissociated and ionized in the discharge and then accelerated into the cathode electrostatically at energies of a few hundred electron volts. The boron delivery rate is controlled independent of the component temperature by the bias voltage and the sub-atmospheric pressure at which the gas is maintained.

Pros:

- Boron ions may gain enough kinetic energy via electrostatic acceleration to penetrate the surface of the component. This should facilitate boron diffusion and result in shorter processing times than those for gas boriding.[6]
- Components do not require external heating if the kinetic energy of the impinging ions is sufficient to maintain the required temperature.[6]
- Component temperatures can be lower (500 °C) than those for previously mentioned processes because the energy for dissociation of the boron-bearing gases is ion-impact driven rather than thermally driven.[40]
- The boron delivery rate can be held constant because decomposition products can be removed as new boron-bearing gas is added during processing.

Cons:

- Gases used for this process are the same as those for gas boriding so concerns about reactivity and toxicity are the same as for that process.[6]
- Treated-layer thickness is a function of surface distance from and orientation with respect to the anode.[6]
- The boron ion delivery rate and energy are difficult to control independently.
- The processing must be done in a pumped and sealed vacuum system.

1.1.5 Conventional Ion Implantation - The boron-bearing gases cited for gas boriding are used in this process by ionizing them in a chamber and then extracting them into an electrostatically accelerated beam.[41-53] In order to remove all but the boron ions

from the beam, it is passed through a magnetic field and a columnator (i.e. a mass separator). As a result of using this device, the beam diameter is generally limited to about one millimeter. In most applications the implantation is done at room temperature, to low doses and at high acceleration energies (100 keV and above). Since no diffusion is involved, it usually results in a thin, amorphous surface layer.[53]

Pros:

- This is a non-equilibrium process, so boron concentrations in the treated surface layer can exceed thermodynamic equilibrium limits.
- Boron delivery through the surface can be controlled precisely at a rate that is independent of the component temperature.

Cons:

- The small beam diameters involved generally require long processing times to treat typical component surface areas.
- The line-of-sight nature of this process limits its usefulness on geometrically complex surfaces.
- The processing must be done in a pumped and sealed vacuum system.
- Mass separation introduces energy and boron utilization inefficiencies and increases equipment costs substantially.
- Gases used for this process are the same as those for gas boriding so concerns about reactivity and toxicity are the same as for that process.
- Beam heating is generally insufficient to raise the surface temperature substantially so diffusion is limited and as a result treated layers are thin (tens of nanometers).

1.1.6 Ion-Implantation Boriding - This process, which is investigated experimentally in this thesis, involves delivery of energetic boron ions through surfaces at temperatures where substantial boron diffusion and boride formation can occur. The implantation system utilizes pure boron (99.99%) that is vaporized, ionized and accelerated into a broad beam that requires no mass analysis.[54] The boron phase produced in a surface layer is controlled by balancing the rates of boron delivery through the surface and diffusion beneath it, by controlling the ion source beam current and the surface temperature, respectively.

Pros:

- The boron delivery can be controlled precisely at temporal rates that are independent of the surface temperature.
- Beam-ion energy, processing time and substrate temperature can also be controlled independently with good precision.
- Beam-ion heating of the component reduces the external-heater power required to sustain its temperature during implantation.
- Environmental concerns associated with corrosive or toxic gases are minimal and solid or liquid waste production is negligible.
- An ion beam with a large cross-sectional area can be used. The 5-cm-diameter beam that will be used in experiments described here is much larger than conventional beams and beams that are larger still are practical.[54]

- Mass separation is unnecessary because ions are extracted from a pure boron plasma.

Cons:

- This is a new process.
- The processing must be done in a pumped and sealed vacuum system.
- As used in the present experiments, this line-of-sight process is useful only for geometrically simple surfaces.

It should be noted that it is possible to use plasma immersion ion implantation [55,56] as a means of overcoming the line-of-sight limitation just cited. For the experimental work described herein, however, the beam process is actually preferred because it affords more precise, wide-range control of the implantation parameters. Independent control of the delivery rate of boron, the substrate temperature and the processing time is important because it enables control of the boride layer composition. This control enables balancing of boron delivery and diffusion rates at values where the preferred Fe_2B phase can be produced. Thus, boron buildup at the surface, which tends to produce brittle FeB layers under many pack, bath, or gas boriding conditions, is avoided. Precise, independent control of the rates of boron supply to and diffusion from an implanted layer near a surface facilitates accurate investigation of diffusion processes that should yield understanding and reveal minimum temperatures at which boron diffusion treatments are practicable.

1.2 Ion implantation boriding versus conventional boriding

An initial objective of this thesis will be to refine the ion implantation boriding process by treating pure α-iron. A goal will be to achieve layer characteristics similar to those associated with conventional boriding. These characteristics include a thick, continuous boride layer with wear characteristics that are much better than those of the non-borided surface. Efforts will be made to avoid high process temperatures, long heat up and cool-down cycles and the formation of the FeB/Fe_2B dual layer. Pure α-iron is used so the effects of boriding can be studied without the interference of any alloying agents.

A parameter that will determine the viability of ion implantation boriding will be the processing time required to create layers of the same thickness as those of the conventional process. Both of these processes involve thermal diffusion and the associated treated-layer thicknesses will be determined by boron diffusion coefficients given by

$$D = D_o \exp\left(-\frac{eH}{k_b T}\right) \qquad (1)$$

where D_O is the pre-exponential coefficient in cm^2s^{-1}, k_b is Boltzmann's contstant (1.38 x 10^{-23} J/K), T is the absolute temperature in K, e is the electron charge (1.6 x 10^{-19} C) and H is the activation energy in eV/atom. Kucera and Stransky [57] give pre-exponential coefficients and activation energies of 2.3 x 10^{-3} cm^2s^{-1} and 0.83 eV/atom for B diffusion in α-Fe and 2.0 x 10^{-3} cm^2s^{-1} and 0.91 eV/atom for B diffusion in γ-Fe when the boron is present at low concentrations (<0.02 at. %).

Diffusion coefficients can also be estimated from the implantation/diffusion time (t in sec.) and the thickness of a treated layer (x in cm) using the equation:

$$D = \frac{<x>^2}{t\beta} \qquad (2)$$

where β is a constant that should have a value near unity. This equation can be used to calculate diffusion coefficients associated with boron diffusion at high concentration levels in iron from published layer-thickness/boriding-time data. [13,29,40,58] Natural logarithms of the diffusion coefficients determined from these data are plotted in Fig. 1 against corresponding inverse temperatures. The reason for plotting these particular quantities becomes apparent when the natural logarithm of Eq. 1 is taken to obtain

$$LnD = LnD_o + \left(-\frac{eH}{k_b}\right)\left(\frac{1}{T}\right) \qquad (3)$$

The solid line in Fig. 1 is the least-squares fit of the data and as Eq. 3 suggests, the activation energy, H, is equal to the slope of this line divided by $-e/k_b$ or 1.21 eV/atom in this case. Also, the pre-exponential coefficient D_O is simply the exponential of the y-axis intercept or 2.5×10^{-3} cm^2s^{-1}. The fact that the activation energy computed from the boriding data is greater than the value published by Kucera and Stransky for α-Fe suggests that boron diffusion rates in the boriding applications are less. This could be a result of a surface impedance or because most of the boron must diffuse through iron borides which have greater activation energies. Data shown by Kunst and Scaaber [59] support the later theory. They show that diffusion of boron through iron borides yields a diffusion coefficient of 1.82×10^{-8} cm^2/s at 950 °C, while diffusion through

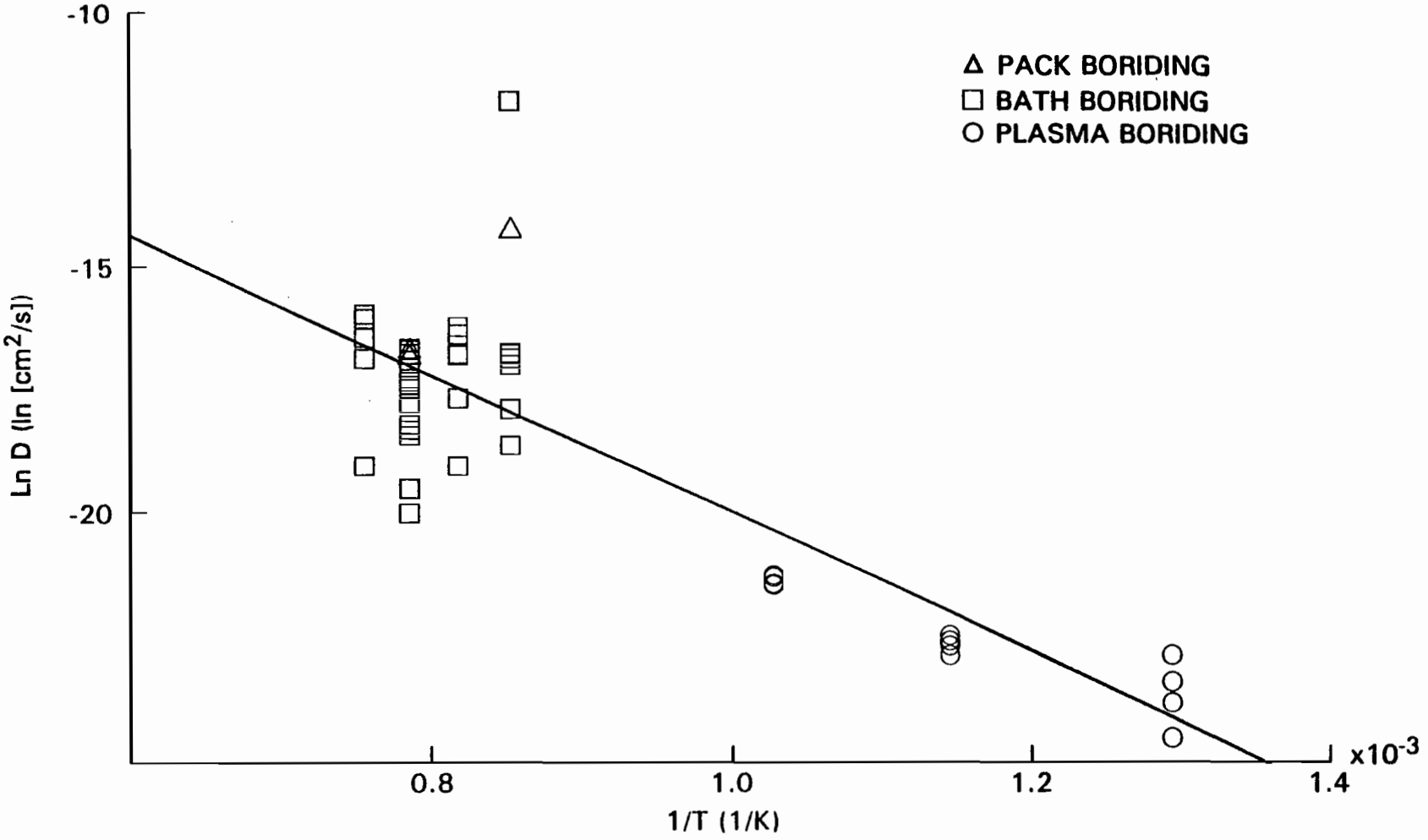

Figure 1 - Diffusion coefficients associated with conventional boriding of α-Fe

iron is an order of magnitude larger, 1.53 x 10^{-7} cm^2/s. Comparison of activation energies and pre-exponential coefficients obtained from ion implantation and these conventional boriding experiments conducted on the α-Fe should give additional insight into the similarity of these two boriding processes.

Although α-Iron is scientifically interesting it sees very little commercial application. For this reason, the effect of ion implantation boriding on the wear resistance of a common tool steel (M2) was also studied. High speed tool steels are used extensively in the manufacturing economy for machining applications including cutting, drilling and milling.[60] It is frequently the sliding wear that occurs on tools that determines their lifetimes and improved wear resistance would extend tool replacement intervals thereby reducing the maintenance part of production costs. Traditional boriding methods have been shown previously to improve wear resistance of other tool steels.[3,6] In this work, implantation boriding was used to diffuse boron into M2 steel and its effect on wear resistance was studied.

2.0 Apparatus and Procedure

Pure α-iron (99.5%) discs with an outer diameter of 4.8 cm, an inner diameter of 1.4 cm and a thickness of 1.83 mm were used for this study. Each disc was polished to a mean roughness of 0.015 μm and cleaned in an ultrasonic bath for 5 minutes in chlorothene and then 5 minutes in acetone just prior to any processing.

Discs were implanted with boron by installing them in the vacuum system which houses a broad-beam, high-current-density metal ion implanter [54] and is shown schematically in Fig. 2. As the figure suggests, each disc was mounted on an electrical resistance heater which was used to raise its temperature to the implantation temperature. During the resistance-heating phase, which required approximately 15 min, each disc was also typically sputter-cleaned and heated by moving the mask so the disc would be exposed to a 20 keV, 500 $\mu A/cm^2$ Ar^+ ion beam extracted from the metal-ion implanter for 3 min. Once the disc was at temperature and the metal ion source was operating on boron, the mask would be positioned so the disc would be exposed to a 20 keV, 500 $\mu A/cm^2$ B^+ ion beam for the prescribed implantation time. During and prior to this time, the disc temperature was monitored using a chromel-alumel thermocouple spot welded to the disc at a point near its outer edge which was shielded from direct ion impingement. This temperature typically rose to the desired value within less than three minutes and was then controlled at the desired value by adjusting the resistance heater power and/or the beam voltage. At the conclusion of the implantation, both the resistance heater and the beam and were turned off and the disc temperature dropped at an initial rate that was typically 65 °C/min.

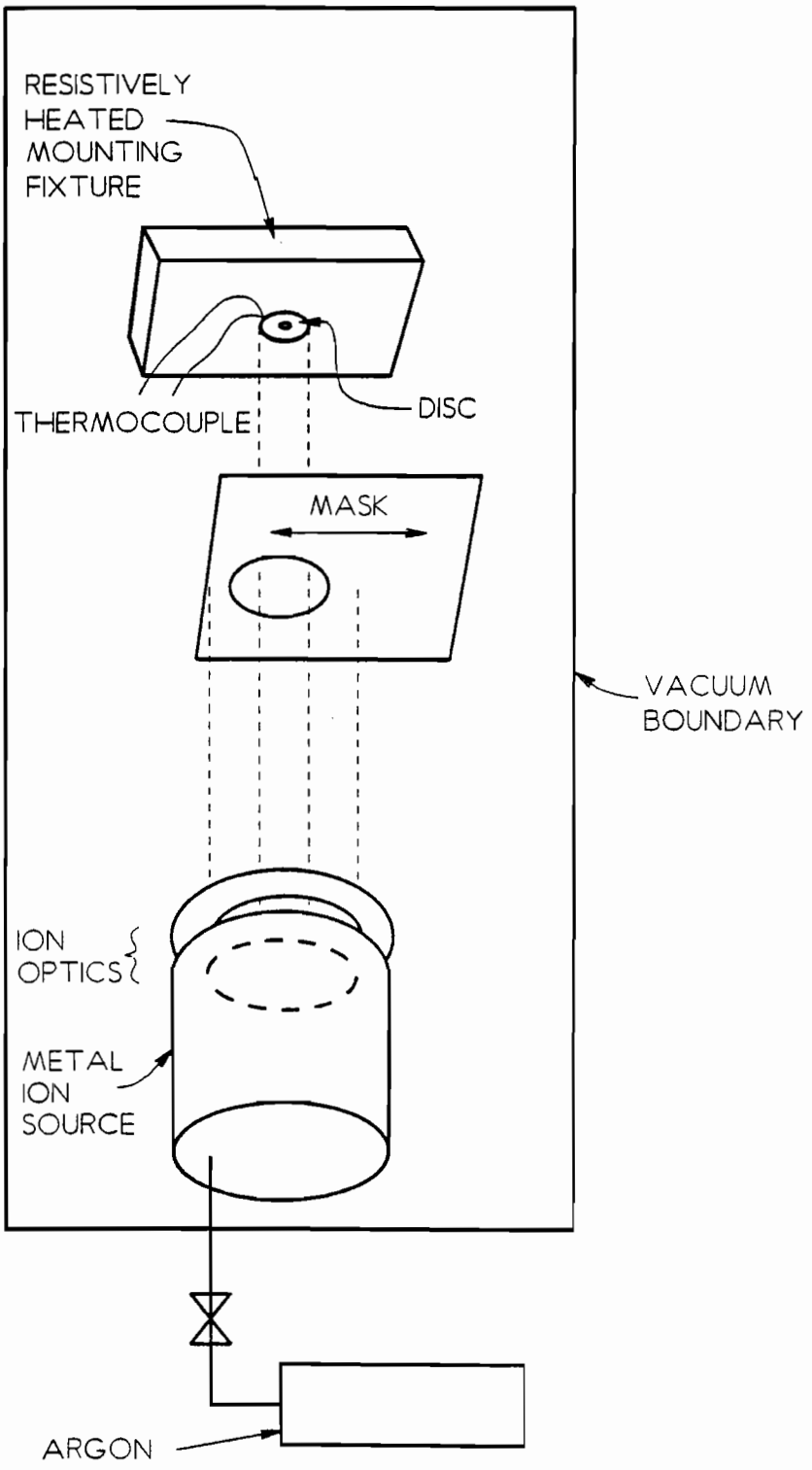

Figure 2 - Implantation system schematic

The boron ion beam extracted from the metal-ion source was derived from a boron plasma which was obtained by vaporizing amorphous boron powder (99.99 %, 300 mesh) that had been pressed into 1 cm diameter pellets and placed in a crucible like that described in Ref. 54. Boron vaporization was accomplished via energetic-electron bombardment of the crucible and the boron pellets within it.

Changes in surface phases induced by the ion implantation boriding of a disc were measured using X-ray diffraction (XRD) spectrometry. This spectrometer, which used CuKα (8 keV) X-rays in the Bragg-Brentano configuration, sensed the conditions in a surface layer that was 1 to 3 μm thick. In some cases the surface was also analyzed with Conversion Electron Mossbauer Spectroscopy (CEMS) and Conversion X-ray Mossbauer Spectroscopy (CXMS) to sense mean phases present in layers that extended to depths of 0.1 and 10 μm, respectively. Boron concentrations were also measured as a function of depth utilizing Auger electron spectroscopy (AES) coupled with sputter erosion. The AES activation region for these measurements was 100 μm in diameter and sputtering was accomplished using a 9 keV, Ar^+ beam at 55° from normal. Boron diffusion depths were generally determined from AES data.

An oscillating pin-on-disk tribometer [61] like that shown schematically in Fig. 3, was used to determine the effects of ion implantation boriding on the wear behavior of the iron discs. This device, which is designed to wear a relatively large area uniformly by repeatedly translating the pin radially inward and outward as the disc is rotated, is well suited to the study of ion-implanted surfaces. For these wear tests a WC pin with a tip radius of 3.17 mm (1/4"), a load of 3.5 N (corresponding to a

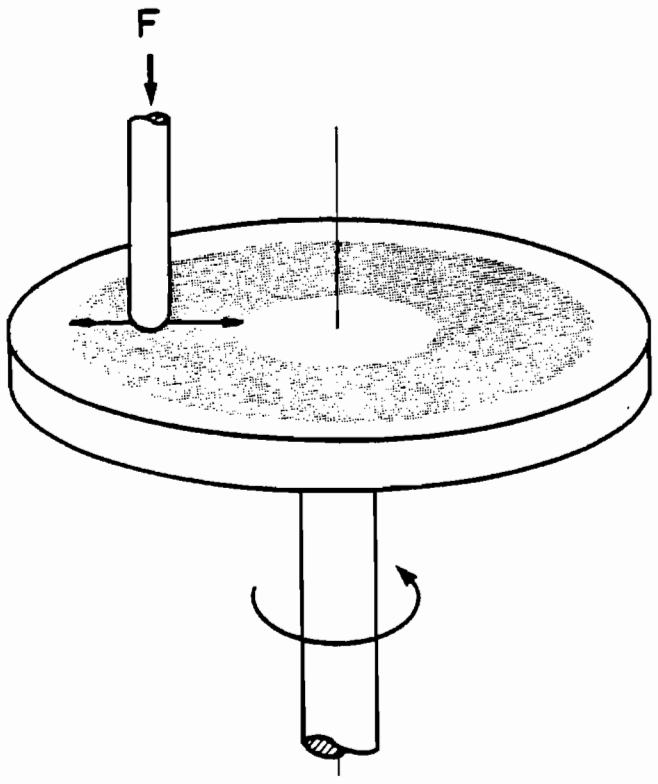

Figure 3 - Pin-on-disc wear tester schematic

Hertzian contact stress of 1.7 GPa), and a mean sliding speed of 0.17 m/s (corresponding to a rotation speed of 100 rpm) were used. The pin and disc were washed continuously with a boundary lubricant consisting by volume of 10 % oleic acid and 90 % kerosene. Disc wear rates were determined by measuring the mass loss as a function of time. The rates were found by removing the samples from the wear test apparatus at prescribed intervals of 0.5, 0.5, 1, 1, 2, 2, 3, 5, 5, 5, and 5 hrs and weighing them on an electronic balance which is accurate to 0.05 mg. Differences in the mean of ten mass measurements were then used to determine the mass-loss history associated with the wear. Optical micrographs were taken of the disc surface before the start of a wear test and after 1 hour of testing.

The M2 steel material (4.4 Cr, 3.0 Mo, 2.3 V, 1.9 W, 4.1 C in at%) used in this study were machined, heat treated and tempered to meet the ASTM specifications for block-on-ring wear testing.[62] The blocks, which were 10.16 mm x 6.35 mm x 15.75 mm, and the rings, which had a 35 mm outside diameter, had final mean roughnesses of 0.25 and 0.3 μm, respectively and both had a hardness of Rc 62.5.

After chemical cleaning, blocks only were placed in the same vacuum system and implanted with the same metal ion implanter [54] as the iron discs. Pairs of blocks were mounted on an electrical resistance heater which was used to preheat and then maintain the blocks at the desired implantation temperature. Before implantation was initiated, the blocks were sputter-cleaned and heated for 3 min. in a 20 keV, 500 $\mu A/cm^2$, Ar^+ ion beam extracted from the metal-ion implanter. The blocks were then masked until implanter operation had been switched to boron and the blocks could

be exposed to the boron ion beam. All blocks were also implantation borided for 15 minutes at an ion beam energy of 20 keV and a beam current density of 500 $\mu A/cm^2$. These blocks were, however, implanted at different temperatures (600, 700, 750, 800 and 900 °C) so the effect of this parameter on the phases that formed and resultant wear behavior could be examined. Rings were not implantation borided.

After implantation the blocks were wear tested on a block-on-ring tribometer like that shown schematically in Fig. 4. The tests were conducted for 1 hour at a relative sliding speed of 0.55 m/s (300 rpm) and a normal load of 222 N (271 MPa Hertzian stress) in a water-soluble boundary lubricant used in maching operations (Long-life 20/20™ which was diluted 20-to-1 with water). The mean wear rate associated with each block was found by measuring the volume lost in its wear scar and dividing it by the test duration. Wear volumes were found from three scar-width measurements [62] and verified using mass-loss measurements.

The implantation borided surface of the blocks was also analyzed with Auger electron spectroscopy and X-ray diffraction.

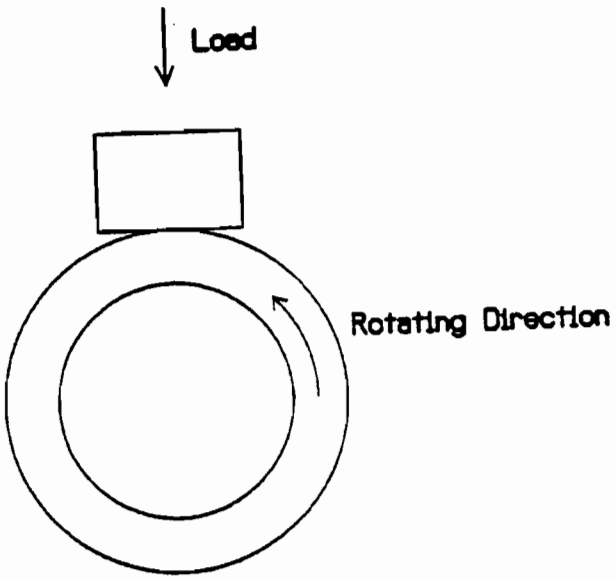

Figure 4 - Block-on-ring wear tester schematic

3.0 Results and Discussion

3.1 α-Iron

It is instructive to examine data obtained from a typical ion-implantation borided disc because similar data were generally obtained on all discs. The α-Fe disc selected was implantation borided at an ion energy of 20 keV, a current density of 500 $\mu A/cm^2$, and a temperature of 700 °C for 15 minutes. This resulted in the boron concentration profile determined using AES that is shown in Fig. 5. It has a maximum concentration near 39 atomic percent and high concentrations that extend to a depth of 0.4 μm before they begin to drop off to a concentration near 10 at. % at approximately 0.8 μm. This plot shows that substantial diffusion has occurred because a TRIM calculation [63] reveals that the maximum depth to which significant boron could be implanted into α-Fe at 20 keV is ~0.05 μm. Because the disc cooled rapidly at the conclusion of the implantation, the diffusion and implantation times are essentially the same.

The dose of implanted boron determined by integrating the AES curve of Fig. 5 to 0.8 μm is 3×10^{18} B/cm^2 and this is equal to the dose determined by the product of beam current density, implantation time and reciprocal of the mean ion charge. The agreement in boron dose determined by these two independent methods indicates essentially all boron delivered during implantation is being retained.

The implanted boron shown to be present by the data of Fig. 5 could exist in one of several phase states. It could have 1) made the iron amorphous as it has been observed to do under low-dose, low-temperature implantation conditions [53], 2) gone into solid solution as nitrogen has been observed to do in stainless steel [64], or 3) it could produce

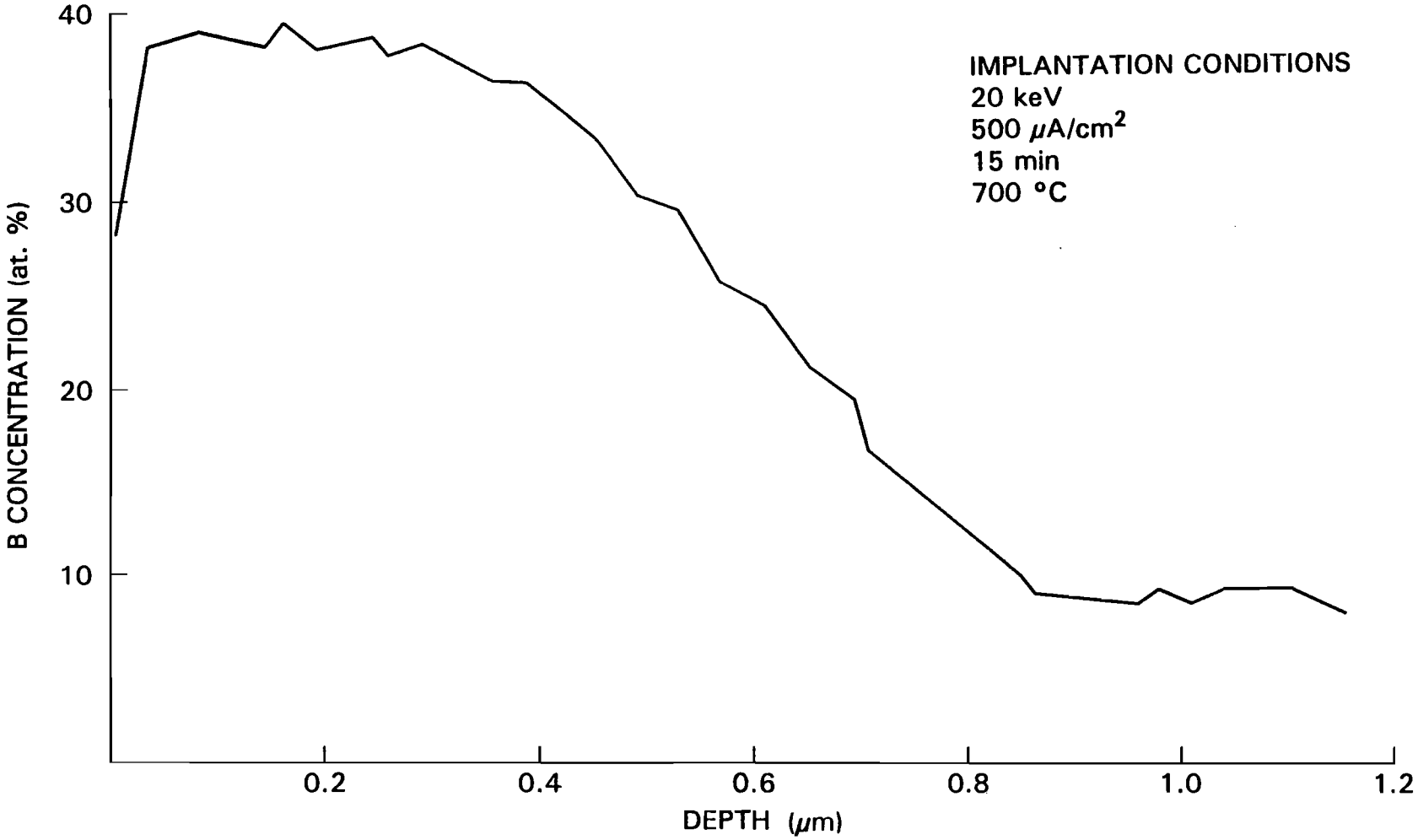

Figure 5 - Boron concentration versus depth for α-Iron ion implantation borided at 700 °C

borides like those produced during conventional boriding and also seen in a preliminary study of ion implantation boriding [65]. The phases that are present within layers of different depths can be determined using XRD, CEMS and CXMS. The XRD data of Fig. 6, which show phases that are present within 1 μm of the surface, indicate the implantation converted what was a completely α-Fe layer into one that is a mixture of Fe_2B, $Fe_{23}B_6$ and α-Fe. These data show no indication of the undesirable FeB phase that makes conventionally borided surfaces brittle. The CEMS and CXMS data of Fig. 7 indicate the phases present in layers that are 0.1 and 10 μm thick, respectively, and they show consistency with the data of Figs. 5 and 6. In the table below the raw data show the strengths associated with the various signals required to match the measured data. Specifically, they indicate that the surface (CEMS data) is essentially all Fe_2B, and that the thicker region (CXMS data) is mostly α-Fe with some Fe_2B and another boride for which Mössbauer data are not available in the literature. This other boride could be the $Fe_{23}B_6$ observed by XRD because Mössbauer are not available for it. The high percentage of Fe_2B seen by CEMS is indicative of a continuous Fe_2B surface layer and the large iron percentage in the CXMS data indicates this layer is not thick compared to the 10 μm sensing depth for CXMS. If one assumes the CXMS signal is coming from a uniform layer of Fe_2B on top of α-Fe, the Fe_2B percentage corresponds to a layer thickness of 1.9 μm. This differs from the thickness of 0.8 μm seen with AES. The fact that 99 percent of the delivered dose of boron is seen in the sample by integrating under the AES curve seems to indicate that the AES is showing the true depth. Both analysis methods were checked [66,67] and no explanation of the discrepancy seems apparent.

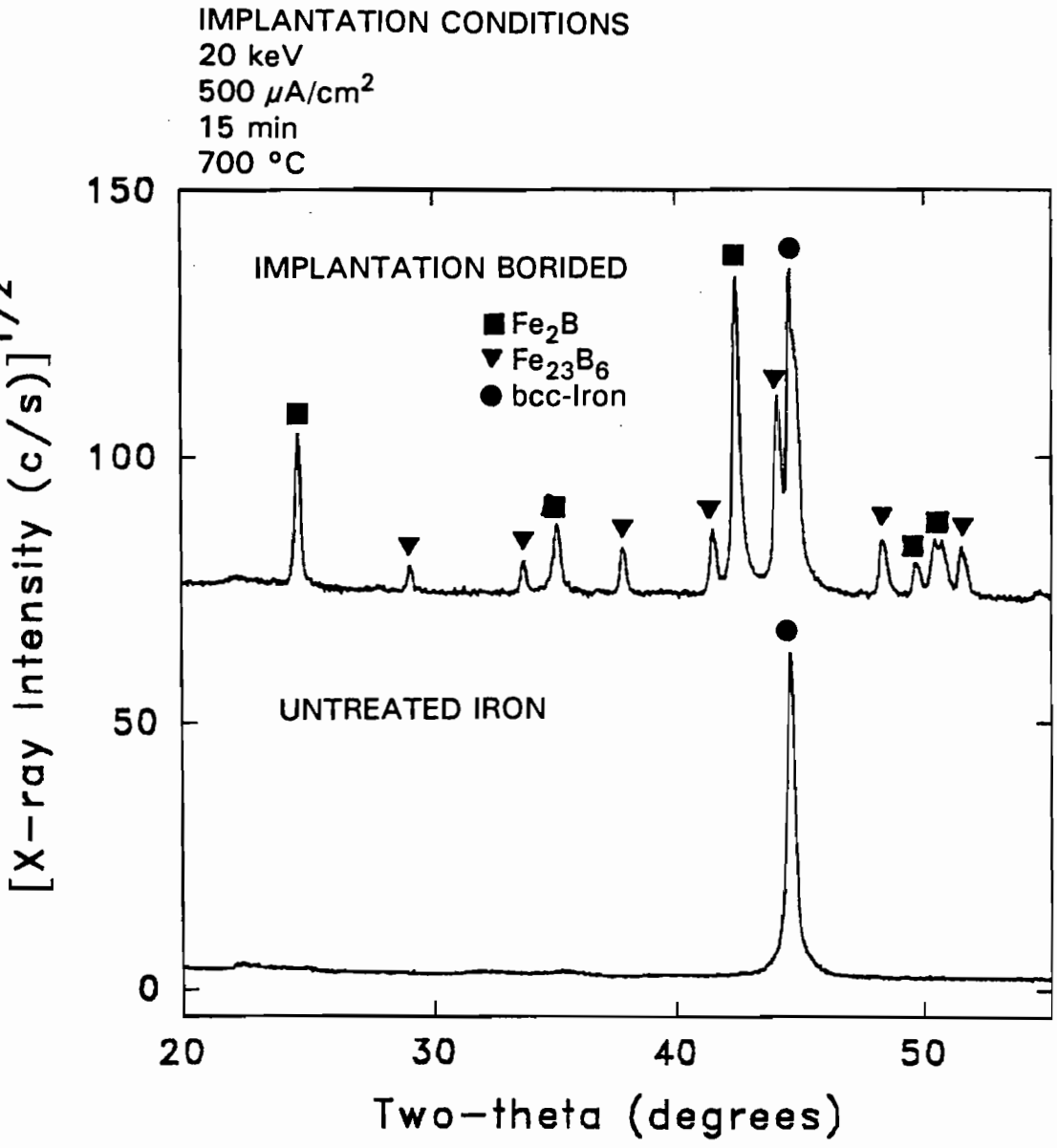

Figure 6 - X-ray diffraction spectra for ion implantation borided iron

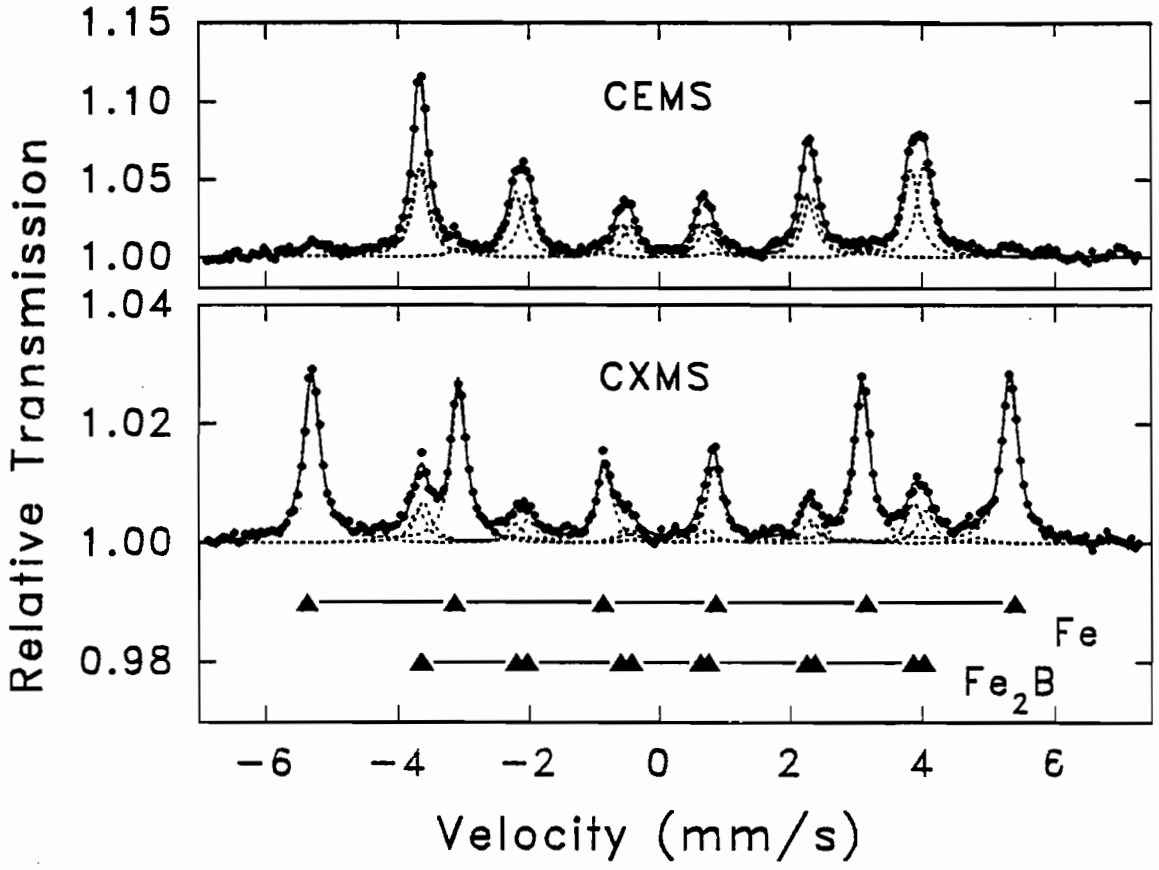

Analysis Method	Percentage Fe_2B	Percentage bcc-Fe	Percentage Fe_xB
CEMS	93	7	0
CXMS	25	72	3

Figure 7 - CEMS and CXMS spectra for ion implantation borided iron

It should be noted that the equilibrium atomic concentration of boron in Fe_2B is 33%. It is believed that the greater B concentration indicated by AES is due to free boron that is trapped while it is in the process of diffusing from the region where it is delivered by implantation to the growth front of the Fe_2B layer. The rapid cooling that occurs after implantation boriding is stopped (65 °C/min) essentially stops the diffusion of boron, thus trapping it in place.

It has been shown that boron diffuses far beyond the depth to which it is implanted at an implantation temperature of 700 °C. In order to understand the diffusion behavior of boron in a material such as iron better, the effect of temperature was examined. This effect was studied by implanting boron at 20 keV and 500 mA/cm^2 into iron at temperatures over the range 600 to 950 °C. The resulting B concentration profiles measured using AES are shown in Fig. 8. They indicate significant diffusion beyond the 0.05 μm implantation depth occurs at all temperatures investigated. They also suggest concentrations near 10 at.% extend deep into the surface at all of the temperatures investigated. Unfortunately, 10 at.% is near the sensitivity limit of these particular measurements, so at least some of these concentrations are probably dropping below this value. At temperatures between 600 and 750 °C the profiles all show similar peak boron concentrations. The 700 and 750 °C AES profiles are similar and compared to them, the 600 °C profile is thinner (~ 0.6 μm). Integration of 600 °C profile in Fig. 8 shows that it corresponds to a boron dose near 90% of the boron that was delivered as determined from the beam current density-time product. These data also show the peak boron concentration drops as the temperature rises above 750 °C. The reason for this is shown in optical micrographs of the surfaces treated at

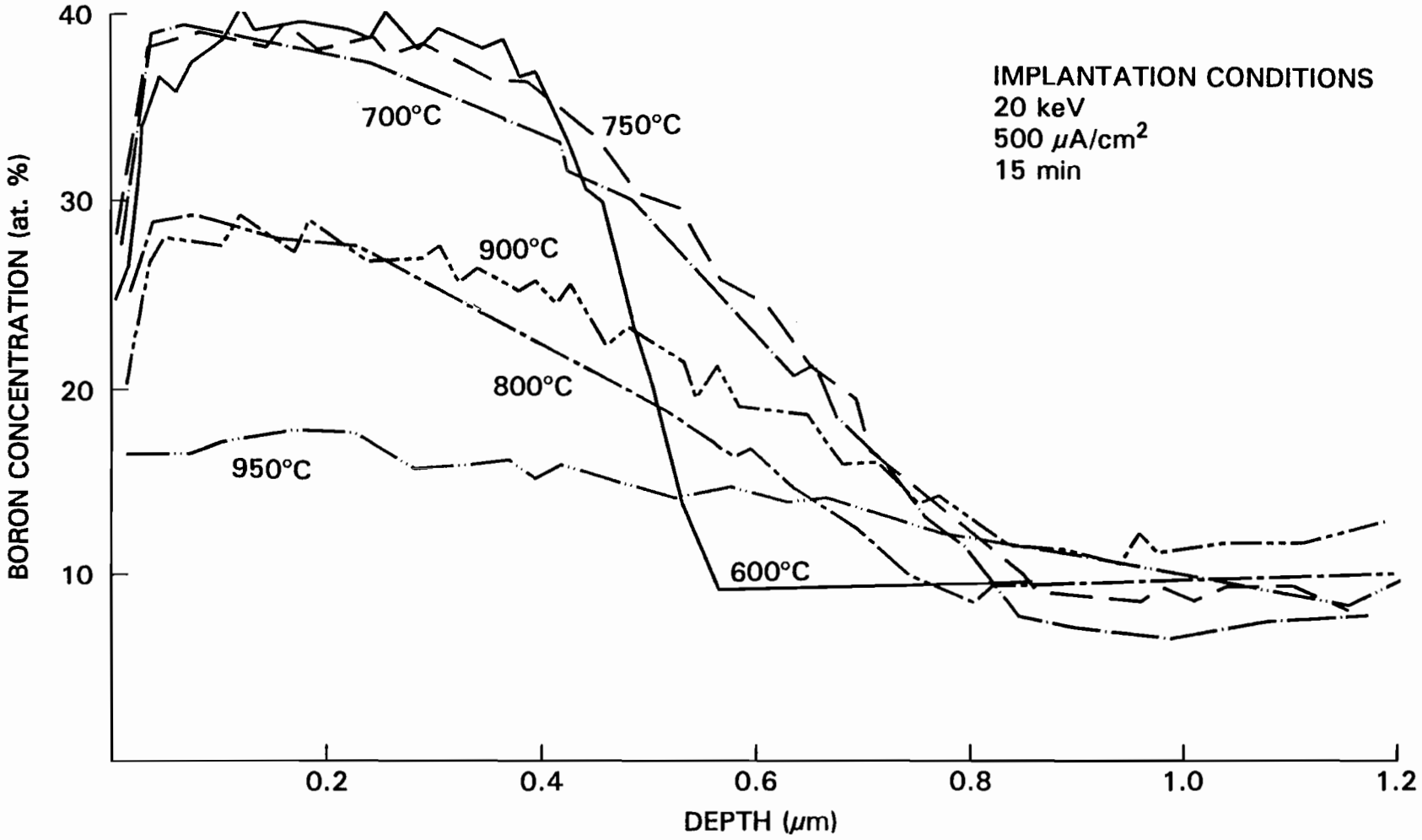

Figure 8 - Effect of temperature on boron concentration profiles for implantation borided iron

700 and 900 °C which are shown in Figs. 9 and 10, respectively. These pictures and CEMS data (72 % Fe_2B, 26 % α-Fe, 2 % Fe_xB for 900 °C) both suggest that the borided surface layer at a lower treatment temperature is continuous while that at the higher one is composed of boride precipitates in an iron matrix. It has been previously shown [65] that these precipitates are Fe_2B. Similar precipitates are seen on the surfaces implanted at 800 °C and 950 °C and micrographs of these surfaces show that precipitate sizes and the separations between them both increase with treatment temperature. It is noteworthy that the AES beam spot used was about 100 μm in diameter so the data of Fig. 8 represent average B concentrations of the Fe_2B/α-Fe matrix in each case. The consequence of the growth in precipitate size and separation for temperatures above 750 °C is, then, the decrease in peak concentrations shown in Fig. 8.

Integration under the AES curves of Fig. 8, for the 800, 900 and 950 °C cases to a depth of 0.8 μm, yields retained boron doses of 65, 65 and 42% of the delivered dose, respectively. Beyond this depth the AES signal drops into the background noise level (10%), and boron concentration values become unreliable. Published activation energy and pre-exponential coefficient data [6, 57] indicate, however, that boron diffuses into iron much more quickly when concentrations are low. This fact coupled with the decrease in retained-dose results suggest that the boron delivered to the surface that is not found in the first 0.8 μm may have diffused deeply into the surface at concentrations below 10%. If it is assumed that the boron concentration remains at 10 at. % for depths 0.8 μm, it is possible to determine the depth to which the boron would have to diffuse to assure all of the B not in

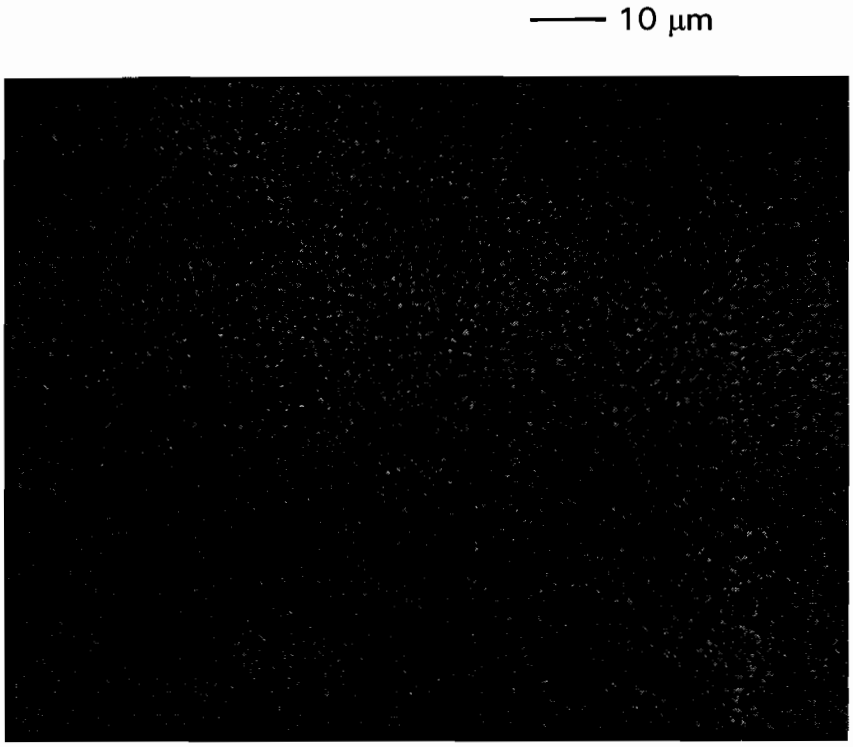

Figure 9 - Iron surface implantation borided at 700 °C (1000X)

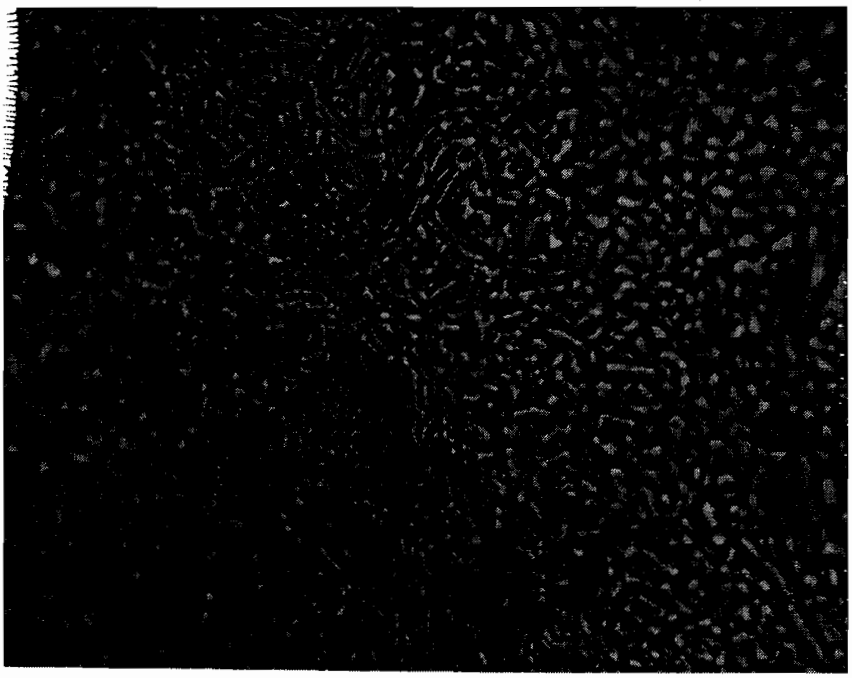

Figure 10 - Iron surface implantation borided at 900 °C (1000X)

the first 0.8 μm is retained . These depths are shown in Figure 11 along with boride-layer thickness' for temperatures of 750 °C and below.

Analyses using XRD, CEMS and CXMS performed on selected surfaces processed over the full range of temperatures were similar in that they showed primarily Fe_2B with some $Fe_{23}B_6$ and no indication of the undesirable phase FeB. At 950 °C, there was also modest evidence of the phase Fe_3B.

The preceding data have shown that iron can be implantation borided and that the phases Fe_2B and $Fe_{23}B_6$ generally form, but the wear characteristics of the resulting surfaces need to be investigated. Raw wear-test results obtained from discs implantation borided at each temperature investigated are compared to the wear behavior of pure iron in Fig. 12. These data, which show disc mass-loss histories over thirty-hour test periods, indicate that all of the implantation-borided iron discs exhibit lower wear rates than the untreated one. The discs implanted in the 600 to 750 °C range exhibit the lowest wear rates in the 10^{-7} $mm^3/N/m$ range, while those at the higher temperatures show wear rates in the 10^{-5} range (Figure 13).

Insight into the reason for the greater wear rates on discs implanted at higher temperatures can be obtained by comparing the optical micrographs in Figs. 14, 15 and 16. They show the surfaces of discs treated at 700 °C after one hour of wear testing and 900 °C after one hour and 30 hours of wear testing. The surface of the disc which has been processed at 700 °C and has the continuous layer, appears the same before and after testing (compare Figs. 10 and 14). Although there is no micrograph of the 700 °C after 30 hours of wear testing the surface continued to look similar to the surface shown in Figure 14. On the

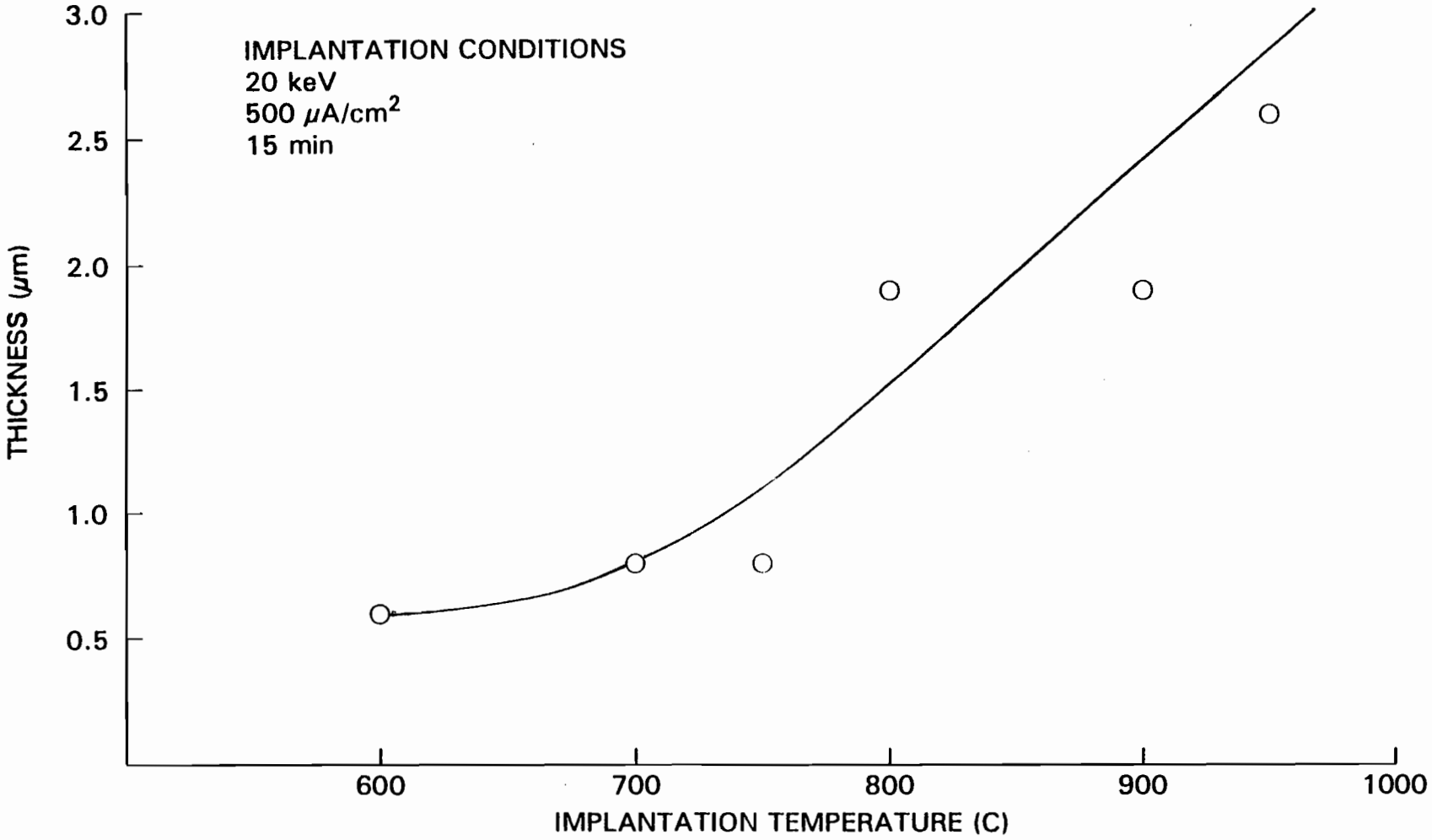

Figure 11 - Boride layer thickness versus implantation temperature in α-Iron

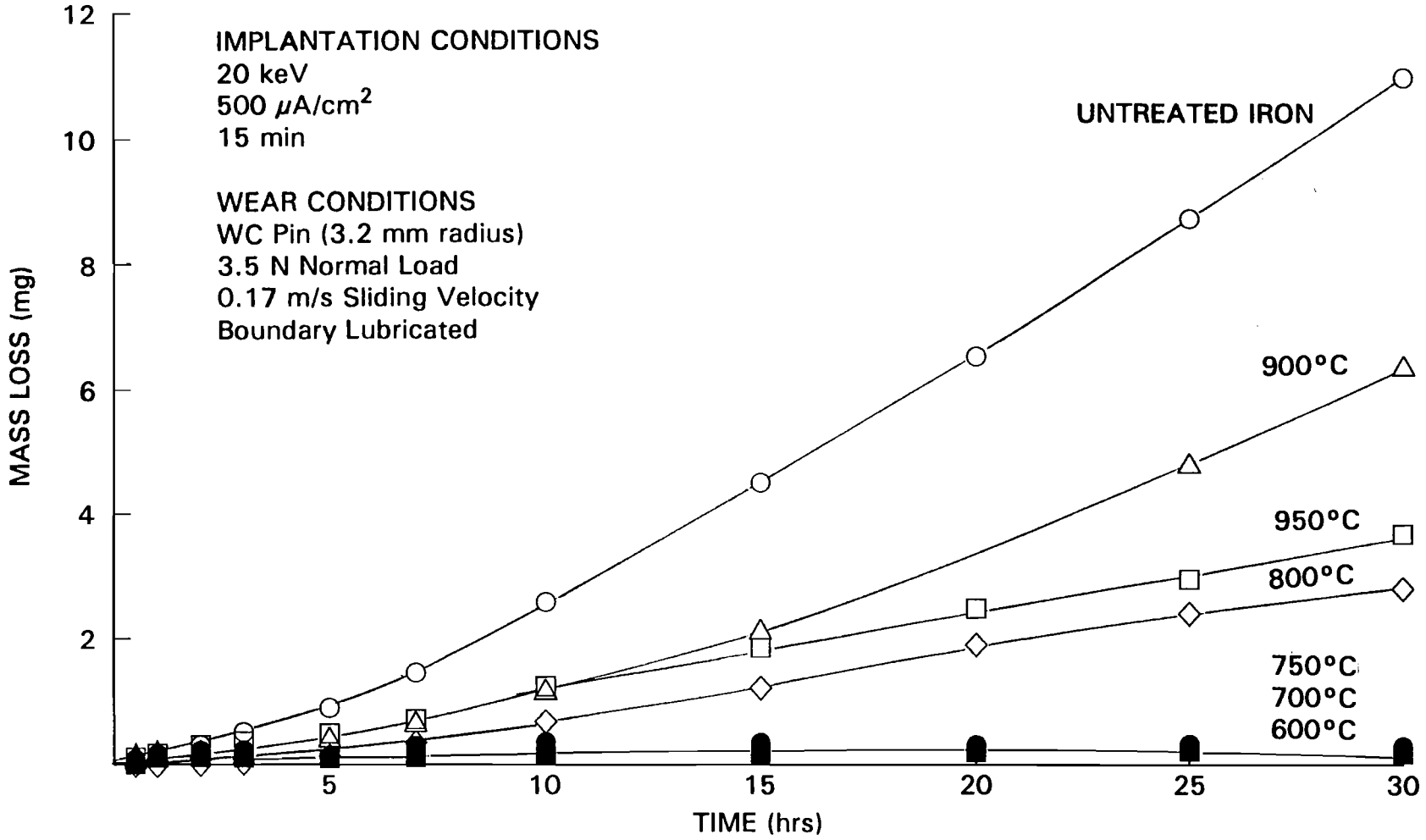

Figure 12 - Effect of implantation boriding temperature on mass loss

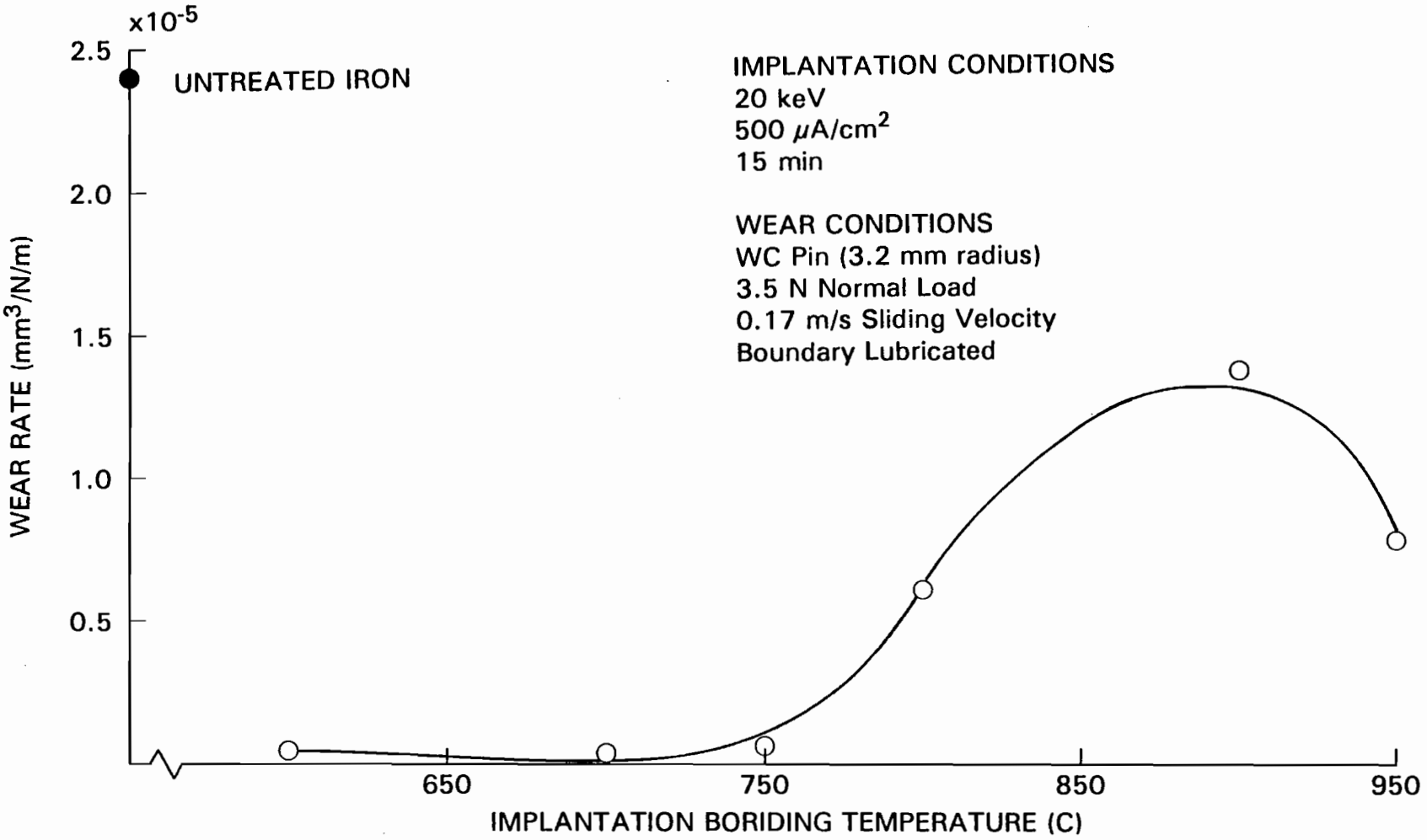

Figure 13 - Wear rates of implantation borided α-Iron

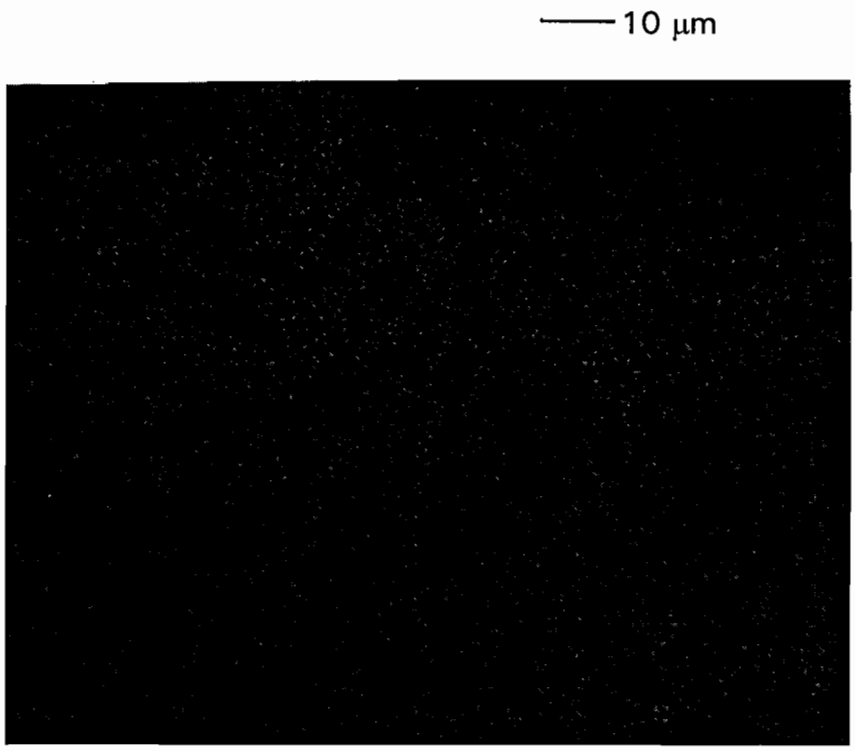

Figure 14 - Iron surface implantation borided at 700 °C after 1 hour of wear (1000X)

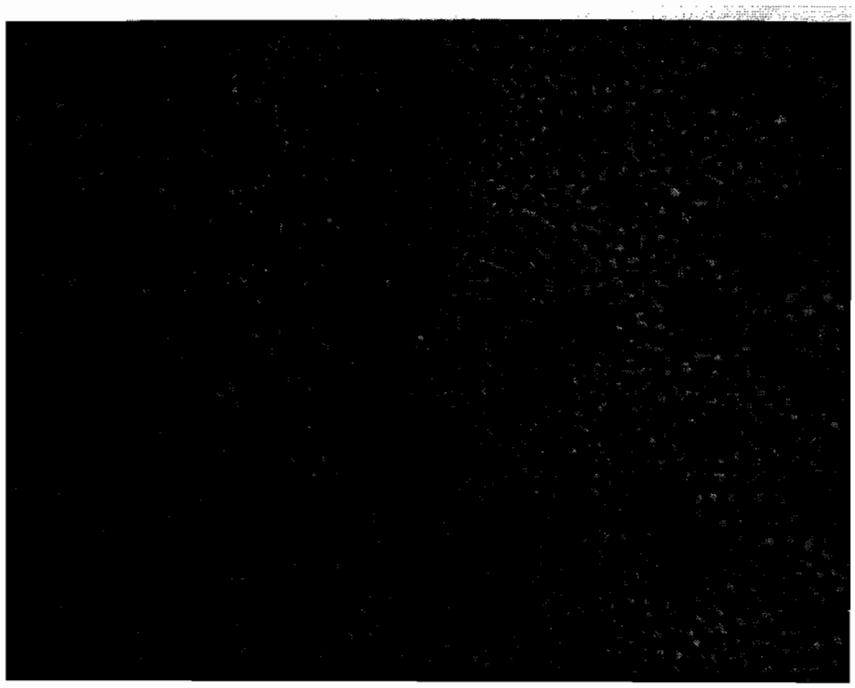

Figure 15 - Iron surface implantation borided at 900 °C after 1 hour of wear (1000X)

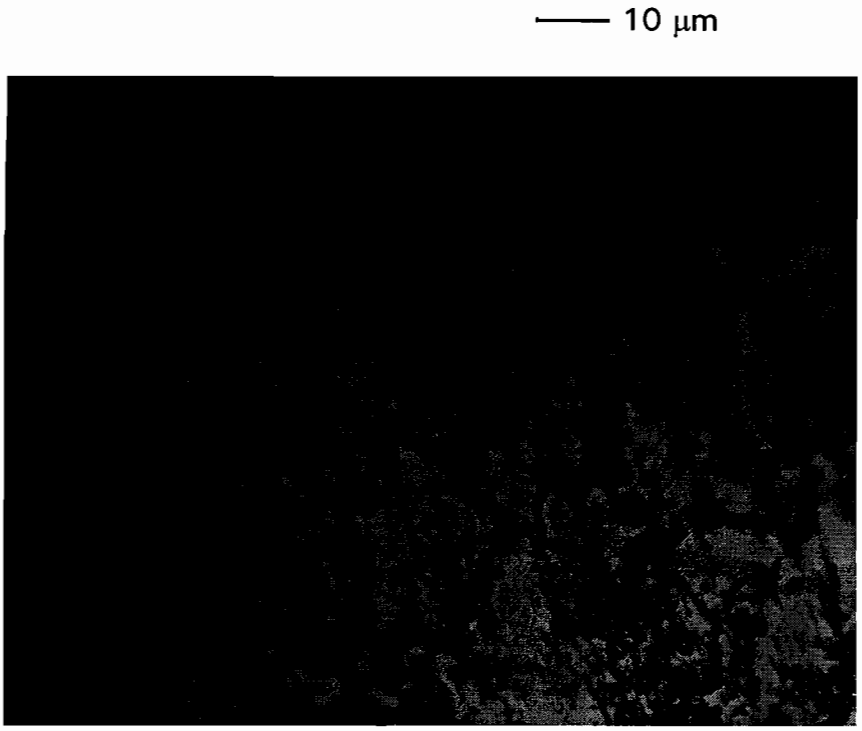

Figure 16 - Iron surface implantation borided at 900 °C after 30 hours of wear (1000X)

other hand, the surface of the one processed at 900 °C shows evidence that the precipitates are pushed into the α-Fe matrix thereby exposing successively more of this matrix to wear (compare Figs. 10, 15 and 16) and producing greater mass-loss rates. This suggests the α-Fe removal rate is determined by the rate at which the precipitates are pushed into the surface of the iron. Strengthening a matrix should reduce the rate of boride intrusion and hence its rate of wear.

The wear data suggest that iron borides in a surface layer are more wear resistant than the iron and that continuous boride layers are still more wear resistant. The continuous layers that have been produced may, however, still not represent the most wear resistant boron-treated iron surface. Traditional boriding techniques continue to show continuous boride layers even when the boriding takes place at higher temperatures than those used here (800 °C - 1050 °C) [3-6,9-25,27-39]. It can be argued that continuous layers are realized at these temperatures because the rate of near-surface boron delivery is sufficient to sustain a boride (Fe_2B) layer in the face of the rates of boron diffusion away from the region of boron delivery. It may be that the precipitates seen on the higher temperature iron samples form as they do because there is a tendency for boron that is implanted into α-Fe to continue to diffuse through the iron while that which falls on an iron boride surface diffuses to a precipitate boundary where it reacts and forms more boride (e.g. Fe_2B).

The rate of boride-layer growth can be quantified in terms of diffusion coefficients, which can be determined using Eq. 2, the layer thickness values of Figure 11 and the processing times corresponding to these values. The results of doing this are plotted as circles in Fig. 17 where the data are presented as the natural log of the diffusion coefficient

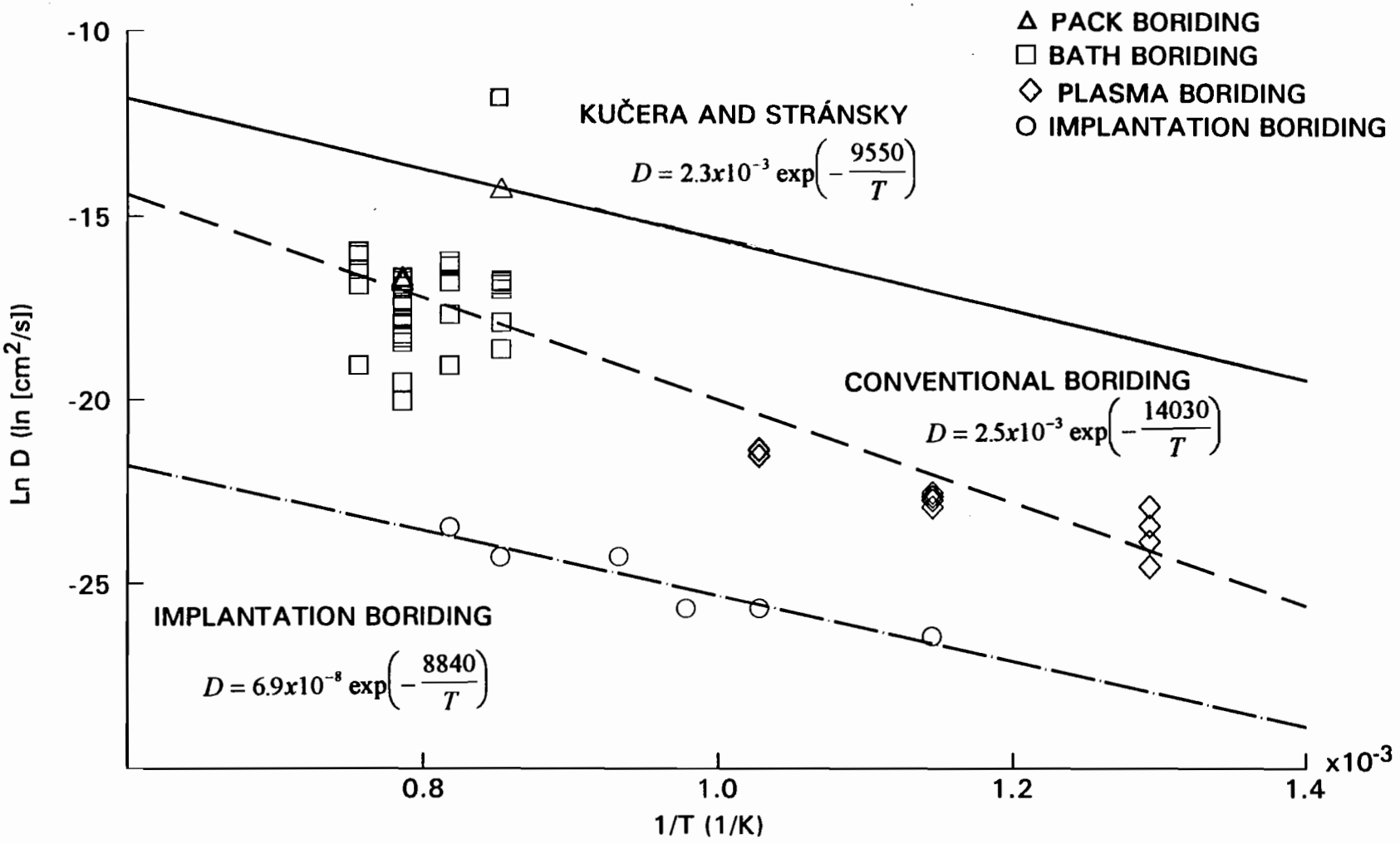

Figure 17 - Diffusion coefficient comparisons

versus inverse temperature. The least-squares fit of these data is shown as the centerline and the activation energy and pre-exponential factor associated with the equation given for this line are 0.76 eV/atom and 7.0 x 10^{-8} cm^2/s, respectively. The conventional boriding data from Fig. 1 and a solid line representative of the Kucera and Stransky results are also plotted for comparison. The lines in Fig. 17 show that boron diffusion as characterized by corresponding diffusion coefficients are 1) high in pure iron [Kucera and Stransky], 2) moderate in iron boride under conventional boriding conditions, and 3) low in iron boride/iron under implantation boriding conditions. The implication of these effective diffusion coefficients is that boron delivered by implantation boriding is probably being limited by the rate of implantation. It is believed that the diffusion behavior of conventional boriding can be approached using ion implantation boriding by increasing ion beam current density. It should, however, be limited to a level where concentrations do not favor the formation of the FeB phase.

3.2 AISI M2

The AES profile measured on the M2 block borided at 700 °C is shown in Fig. 18. Except for an irregularity in the first 0.1 μm this profile has the shape that would be expected for a case where boron is delivered near the surface and it diffuses into a boron-free region. The AES profile shows concentrations that drop from over 40 at.% at the surface to approximately 10 atomic percent (where the AES accuracy becomes marginal) at a depth near 0.55 μm. Because this depth is much greater than the calculated ballistic depth [63] of 0.05 μm, it is obvious that substantial thermal

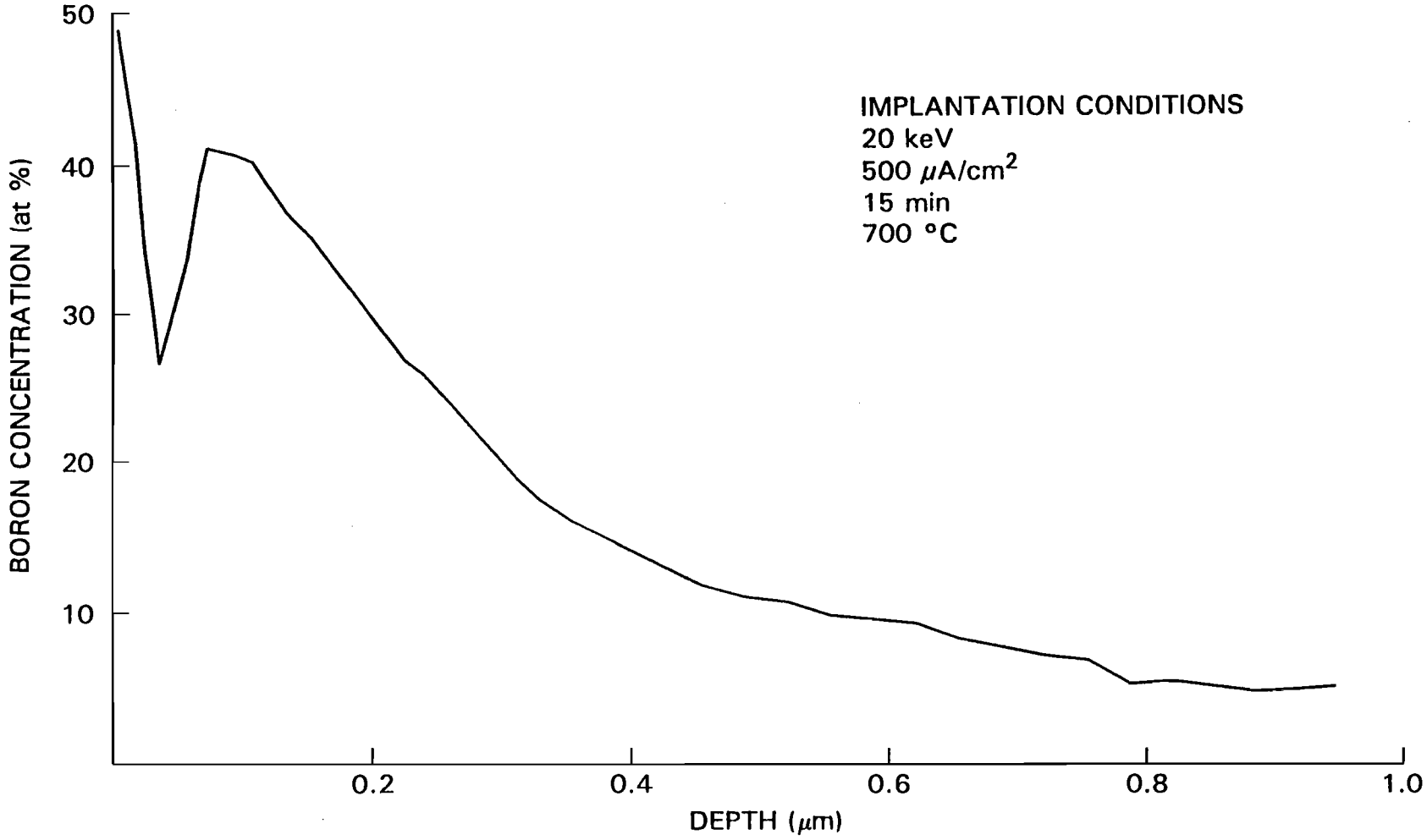

Figure 18 - Boron concentration profile for implantation borided M2 tool steel

diffusion has occurred. It is noted that the diffusion depths of Fig. 18 are less than those associated with the pure iron implantation borided at this temperature. It is suggested that this is the case because alloying agents in the M2 steel inhibit boron diffusion. This result is consistent with the work of Sampsonov and Epik [27] who found that carbon, chromium, tungsten, molybdenum and vanadium all inhibit boron diffusion during conventional boriding. They found that even small percentages of these elements can have a profound effect, e.g. 1 at.% of tungsten can reduce the layer thickness by up to 50%.[27] Goeuroit, et al. [18] confirm that carbon and chromium lower the thickness of a borided layer and Carbucicchio, et al. [12,19,24] observe similar effects.

Surface analysis by XRD allows a comparison of phase changes induced in a layer as the implantation boriding temperature is varied. As with pure iron, the only borides shown in the XRD spectra of Fig. 19 are $Fe_{23}B_6$, Fe_2B and for the block implanted at 900 °C, Fe_3B. None of the brittle FeB phase is observed. Comparison of the unimplanted and 600 °C spectra suggests implantation boriding at this low temperature induces the formation of no boride phases, although the V_4C_3 peak is greatly diminished. The lack of borides at 600 °C could be related to amorphization [68] or insignificant B diffusion leading to a treated layer that is so thin that XRD signals from it are insignificant compared to those from the rest of the 1-μm-thick region sampled by this analysis technique. It is considered significant that small Fe_2B signals are seen in blocks implantation borided at 700 °C and 750 °C but not in those treated at 800 °C and 900 °C. This suggests that the boron is diffusing sufficiently fast

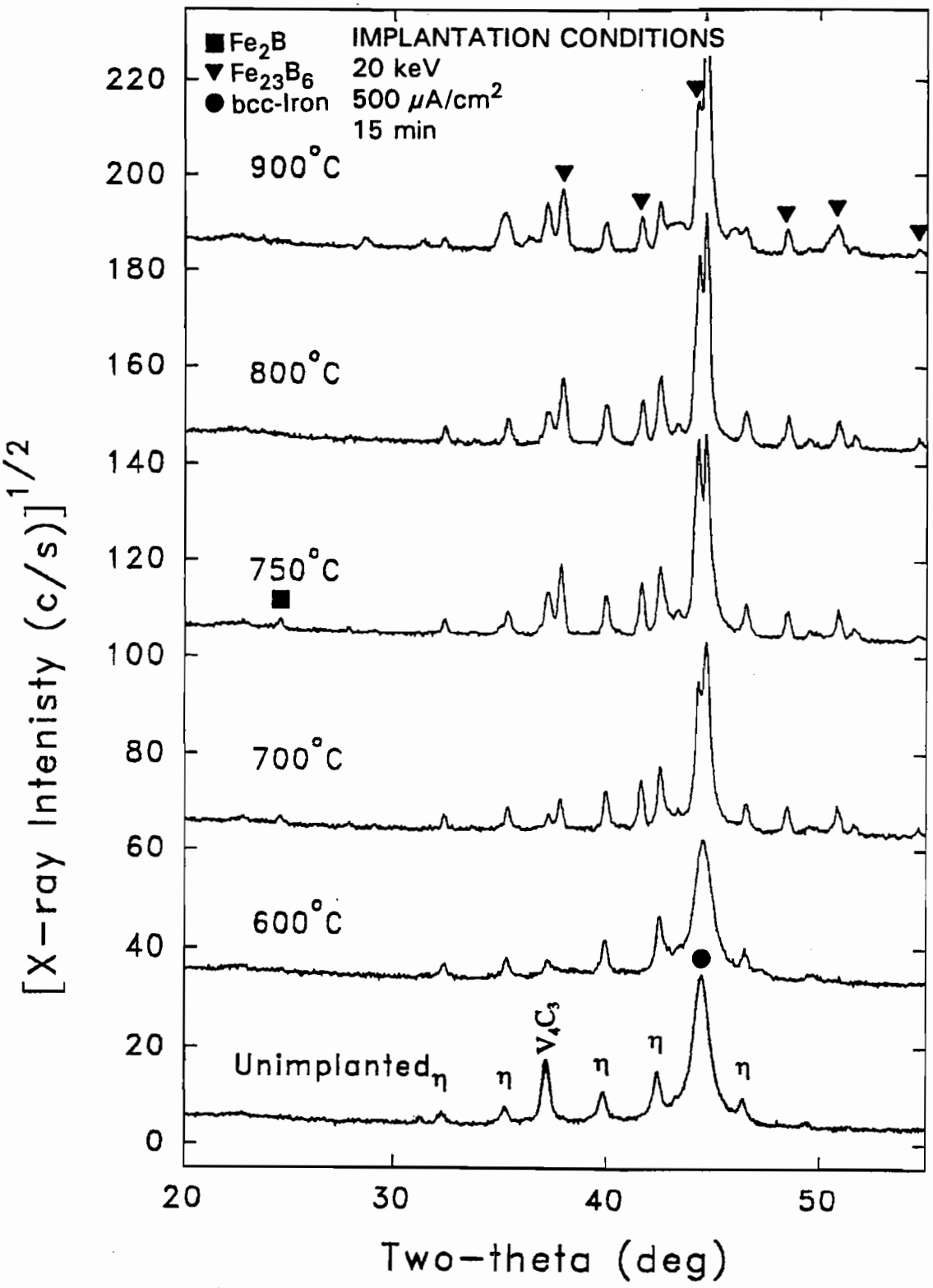

Figure 19 - X-ray diffraction spectra for implantation borided M2 steel

at the higher temperatures so that the phases with lower B concentrations ($Fe_{23}B_6$ and Fe_3B with 20 at.% B and 25 at.% B, respectively) form in preference to Fe_2B (33 at.% B).

Effects of ion implantation boriding temperature on the sliding wear behavior of M2 steel blocks worn against M2 steel rings are shown in Fig. 20. Because the implantation boriding temperature could also affect the properties of the bulk material and this could also influence wear behavior, two sets of data are plotted. The dashed line shows that the wear rate behavior of implantation borided steel blocks remain relatively constant, then rises and drops as their processing temperature is increased from 500 to 900 °C. The solid line shows the effect of the same temperature history experienced by the implantation borided blocks if no boron is supplied. These data were obtained from unimplanted sides of the blocks that yielded the dashed-line data of Fig. 20 so surfaces associated with corresponding temperatures should have experienced about the same thermal history. The results show that wear rates are about the same at the lower temperatures where no borides are formed (up to 600 °C). Blocks implanted at temperatures where the data of Fig. 19 show borides formed, have up to 27% lower wear rates than corresponding unimplanted blocks. The data of Fig. 20 also show that untreated blocks exhibited wear rates that are lower than those for both the implanted and thermally cycled blocks. The reason for this is uncertain, but the corresponding Vicker's hardness data of Fig. 21 provide some additional insight into the wear behavior shown in Fig. 20. These data suggest that 1) exposure to temperatures above approximately 600 °C induce softening of M2 steel whether or not

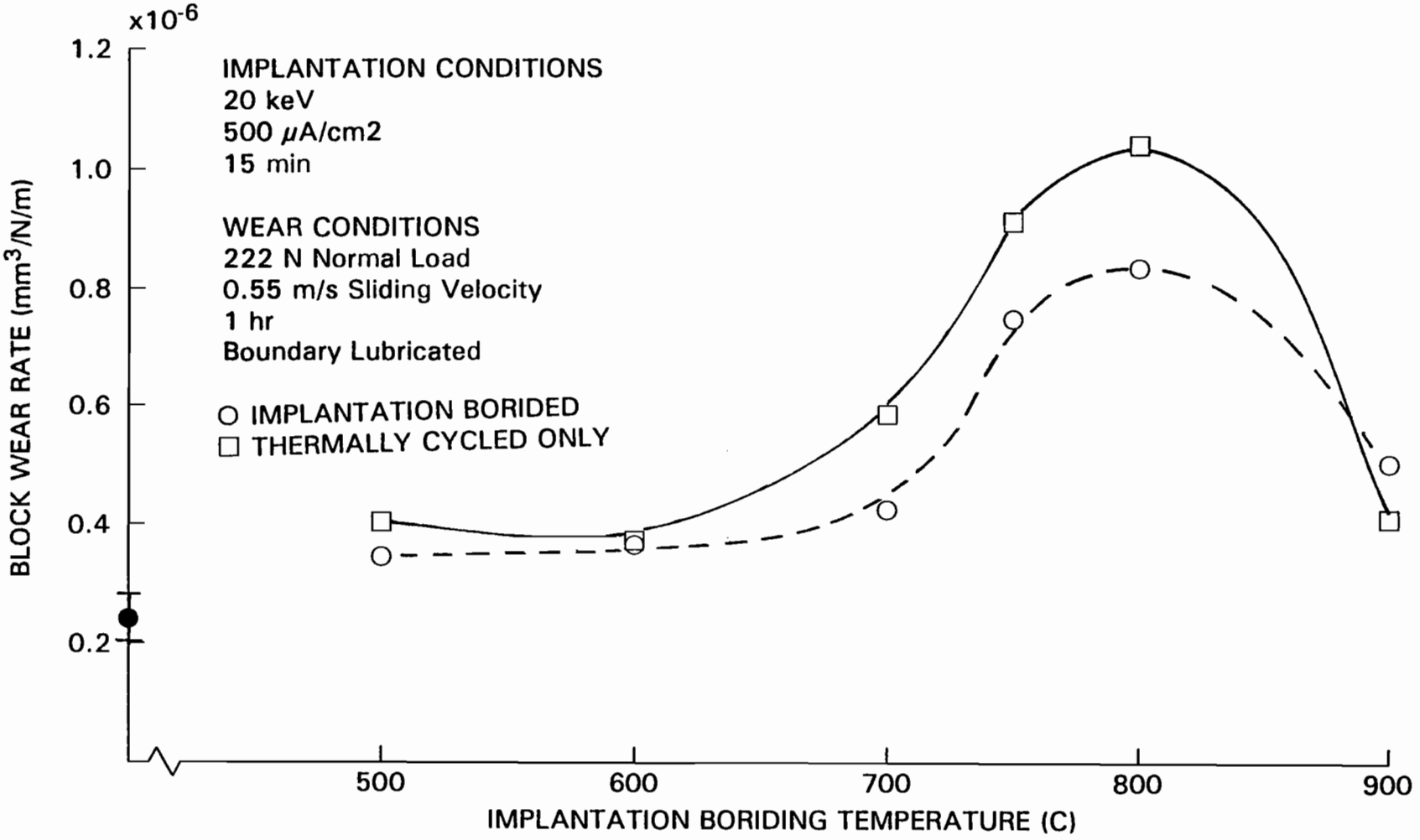

Figure 20 - Effect of implantation boriding temperature on wear rate of M2 steel

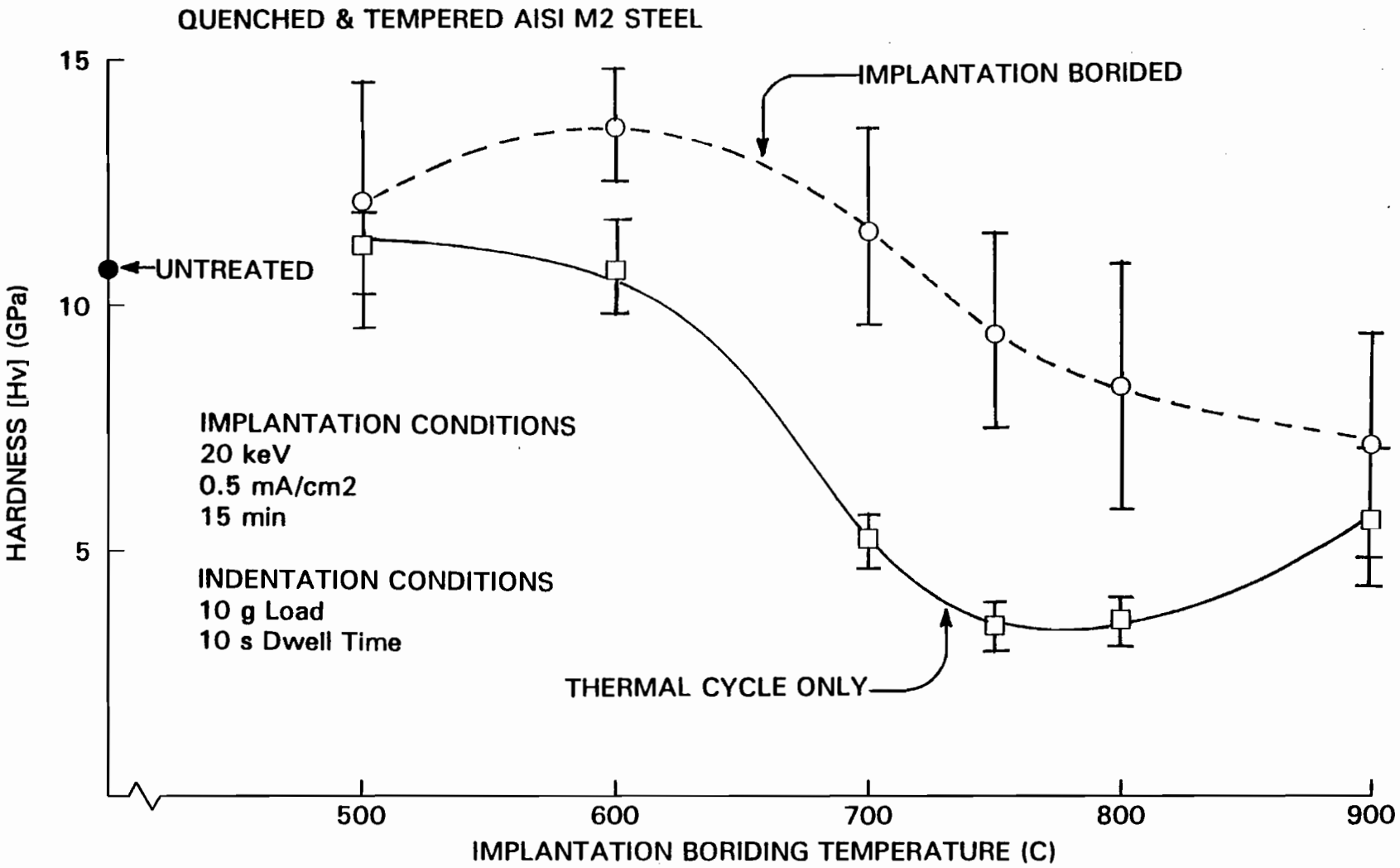

Figure 21 - Effect of implantation boriding temperature on hardness of M2 steel

B is supplied, 2) introduction of B into a thermally cycled surface makes it harder than one subjected only to thermal cycling, and 3) implantation boriding at a temperature less than about 600 °C makes a surface marginally harder than the untreated material.

Taken together, the data of both Figs. 19 and 21 suggest that the boride formation and surface hardening associated with implantation boriding is complicated by the thermal cycling of the bulk M2 steel beneath the treated surface that accompanies the process. If temperatures and normal wear loads are both great enough, this can result in sufficient subsurface softening so that boride precipitates can be pulled from the surface as the wear proceeds and surface mass can be lost more rapidly than it would be from the untreated surface. It appears that this occurs because bulk material annealing takes place when temperatures are above approximately 600 °C for a sufficient length of time. As processing temperatures are raised above 800 °C, however, the data suggest that the wear rate and hardness effects begin to reverse themselves. At a processing temperature of 900 °C, wear rates have dropped back to the point where they approach those associated with 500 to 600 °C temperatures.

A reason for the improvement in wear behavior as the processing temperature approaches 900 °C may be understood by considering the continuous cooling transformation diagram for M2 steel which is shown in Fig. 22 [69]. It shows that the austenite-to-ferrite transition, which is associated with the A 90% and A 10% lines in the figure, occurs in the temperature range 820 to 880 °C. The figure also shows the 900°C-block cooldown path misses the bainite nose at ~300°C and 1200 sec. Thus, it appears that the blocks implanted at and thermally cycled to 900 °C both form some

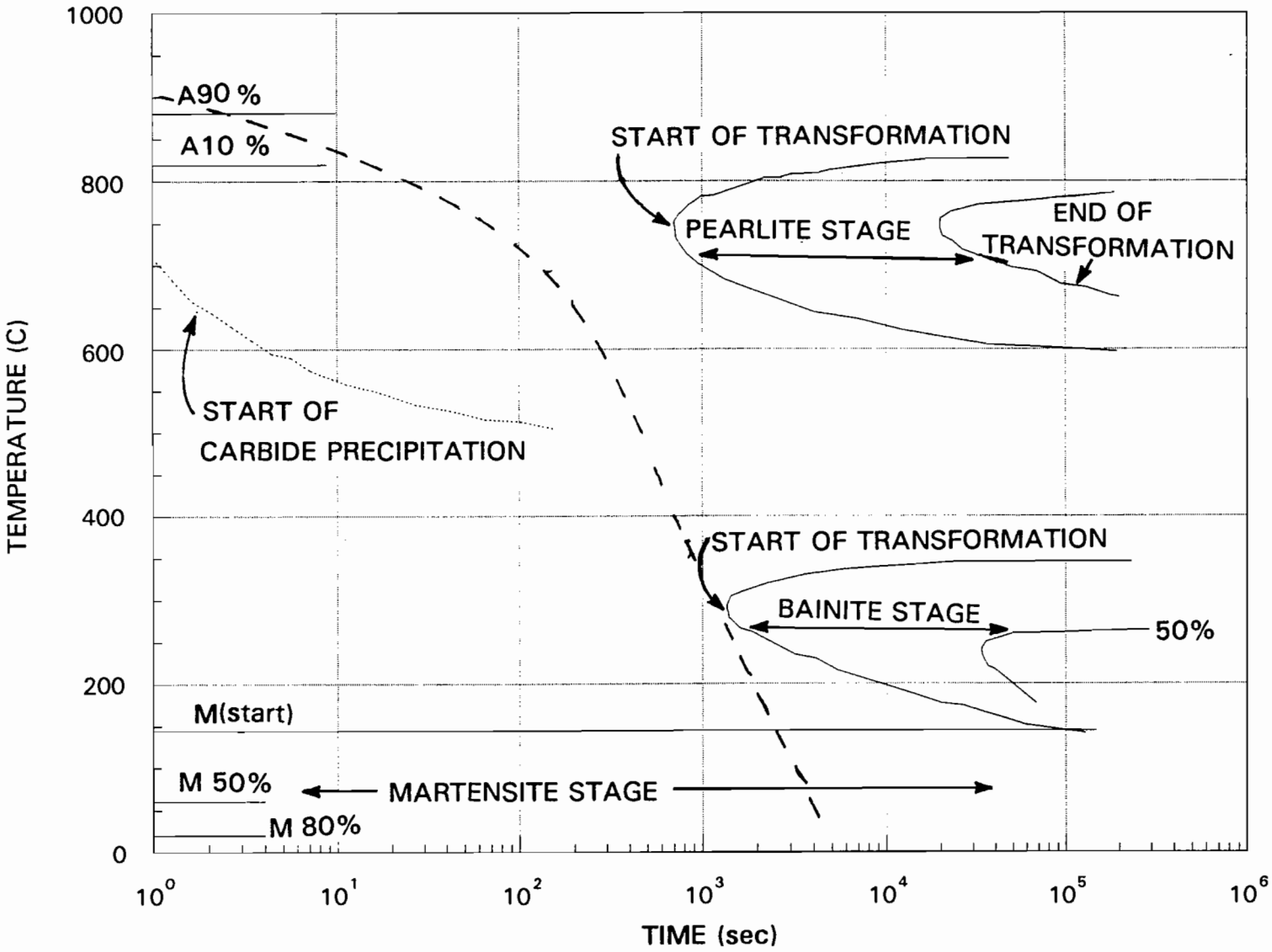

Figure 22 - Continuous cooling transformation diagram for M2 steel
(Reprinted with permission [69])

austenite when they are at high temperature and then undergo martensitic transformations on cooldown that yield bulk materials that are harder than those processed in the 700 to 800°C temperature range. The resulting bulk hardening may still not be as effective as that associated with the original heat treatment because the processing temperature was substantially less than the recommended austenitizing temperature of 1210 °C.

Blocks were examined after being wear tested by etching them in 3% nital for 60 sec and then examining the etched wear scar under an optical microscope. When this was done, the light area shown at the edge of the wear scar in Fig. 23 was observed. This particular micrograph was obtained on the block implantation borided at 800 °C, but those treated at 700 and 750 °C are similar. Auger electron spectroscopic analysis was done at the 4 different points on and near the the light area shown in Fig. 23 to determined boron concentrations. It revealed that B concentrations were 19% at points 1 and 2 and negligible at points 3 and 4. This suggests that the light area is a boride layer and there is little to no boron below this layer.

The thickness of the boride layer (d) can be determined from the width of the light area (x) using the equation

$$d = \left(r^2 - (c-x)^2\right)^{\left(\frac{1}{2}\right)} - \left(r^2 - c^2\right)^{\left(\frac{1}{2}\right)} \qquad (4)$$

where c is half the width of the wear scar and r is the radius of the wear ring. Optical microscope measurements of x were made at 10 different places across the wear scars

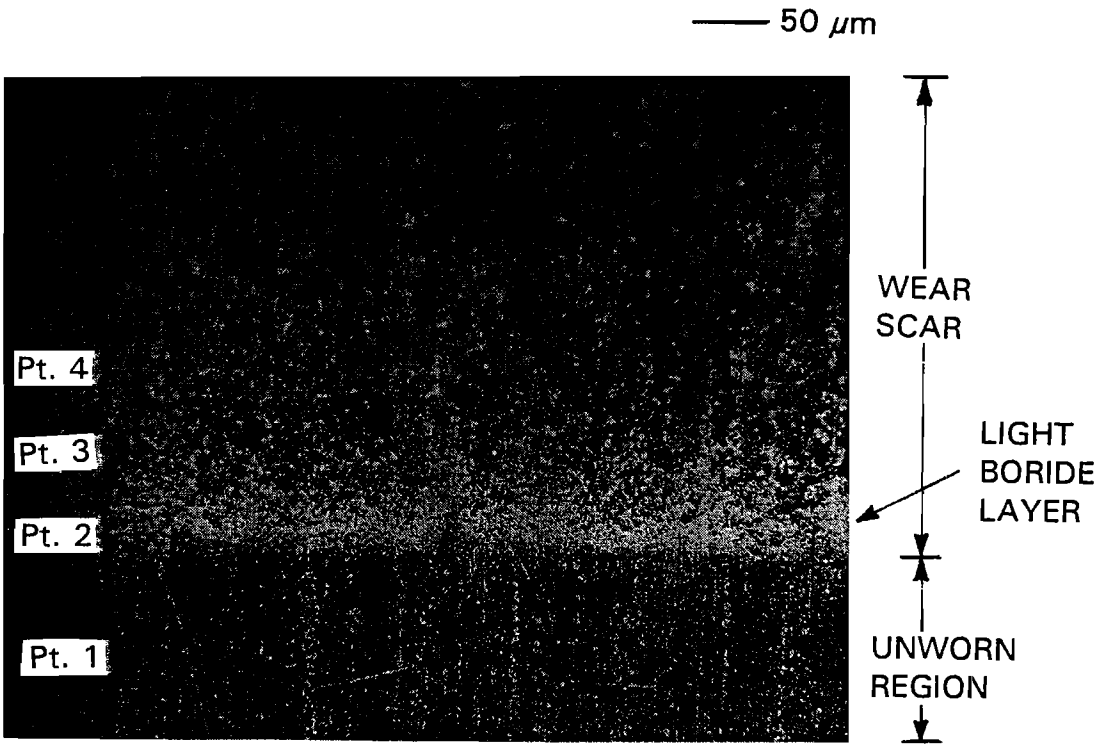

Figure 23 - Optical micrograph of M2 steel implantation borided at 800 °C (Edge of wear scar at 200X)

for each of the implantation borided blocks on which white regions were visible. Using these values in Eq. 4, thicknesses of 0.7, 1.0 and 1.6 μm were computed for the blockstreated at 700, 750 and 800 °C, respectively. These thicknesses were used in Eq. 2 along with the implantation time of 15 min to compute diffusion coefficients. The natural logrithms of the resulting coefficients are plotted against reciprocal temperature in Fig. 24. The slope and y intercept of the line through these data correspond to an activation energy of 1.48 eV/atom and a pre-exponential coefficient of 8.93×10^{-5} cm^2/s. This activation energy is greater than that for boron in iron [57] or boron through iron boride as seen earlier.(Figure 1)

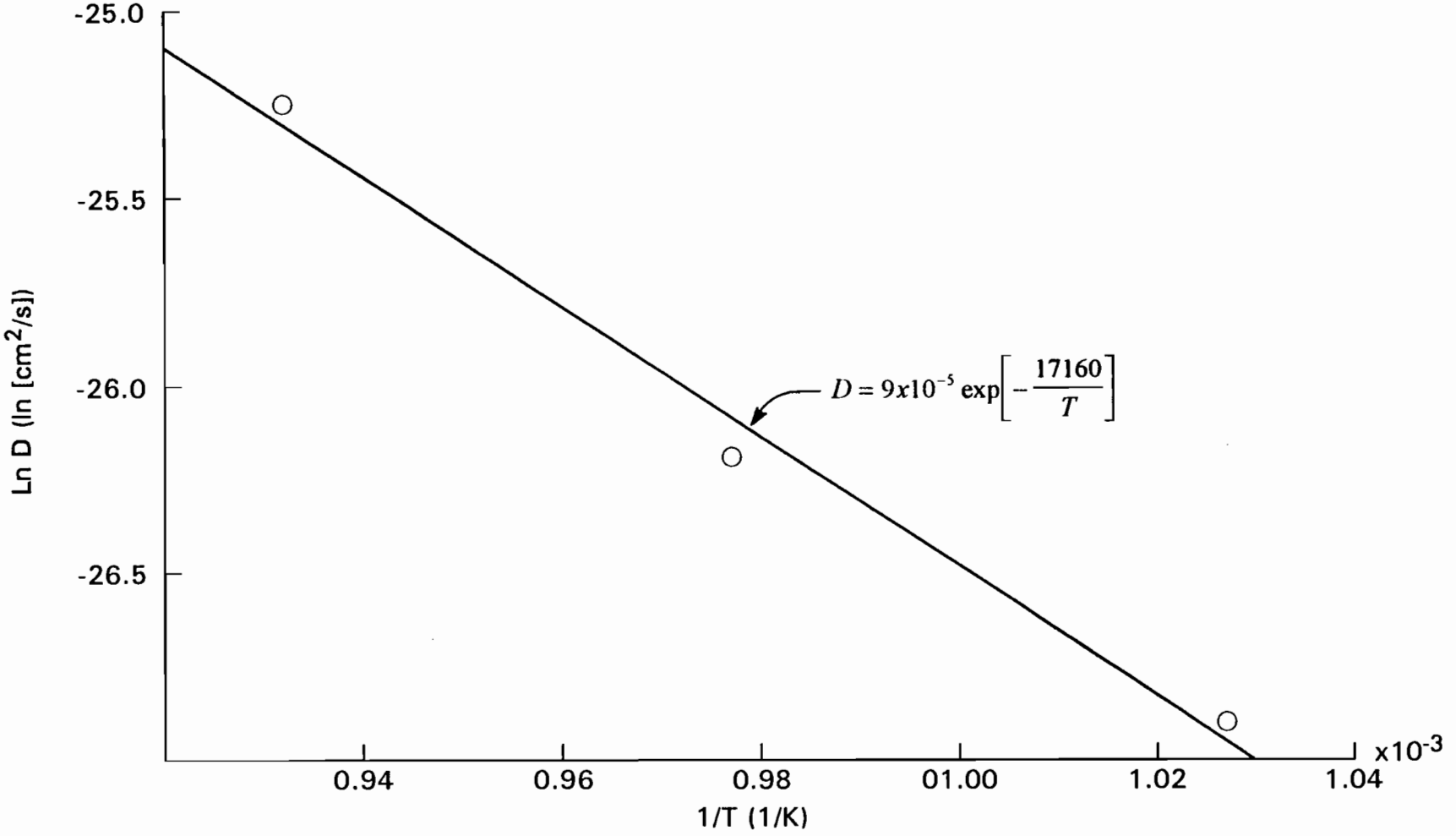

Figure 24 - Diffusion coefficients/reciprocal temperature plot for implantation boriding of quenched and tempered M2 steel

4.0 Conclusions

The Colorado State University metal ion implanter can be operated on pure, solid boron. Boron ions can be extracted and implanted at current densities equal to or greater than 500 mA/cm^2 over about a 5 cm diameter region. Relatively stable operating conditions can generally be sustained for a period of about 15 min although operation was maintained for 45 min. on multiple occasions. Independent control of the temperature of a target surface can be maintained over the range 600 to 950 °C during implantation and temperatures in this range are sufficiently high to enable ion implantation boriding of an iron surface at an implantation energy of 20 keV. The theoretical ballistic depth of boron implanted into iron under these conditions is ~0.05 mm but thermal diffusion in this temperature range induces at least order of magnitude greater depths. There is evidence that boron may diffuse even several times this deep at moderate concentrations ($< 10\%$).

Ion implantation boriding of iron at the conditions of this study generally yields only the phases Fe_2B and $Fe_{23}B_6$ at all substrate temperatures studied. Under no conditions was the brittle phase FeB, which is usually formed with conventional boriding techniques, observed. Over the temperature range 600 to 750 °C the boride layers appeared to be continuous and the resulting surfaces were much more wear resistant than the discrete, 10 micron-sized boride precipitates in an α-Fe matrix which formed at greater temperatures.

Ion implantation boriding does not yield boride-layer growth rates as great as those observed with conventional boriding techniques. Increases in the boron ion current density are considered readily achievable with the existing equipment and they should lead to boride layer growth rates approaching those of conventional boriding techniques.

Boron-rich layers produced on M2 tool steel surfaces by implantation boriding them at 700 to 800 °C are several times as thick as the computed ballistic depth associated with the implantation energy (0.05 μm). This indicates substantial thermal diffusion occurs at these temperatures. At the 20 keV, 0.5 mA/cm^2, 15 min implantation conditions used for this work, the layer appeared to be amorphous at temperature below 700 °C and the borides $Fe_{23}B_6$ and Fe_2B were formed at temperatures at and above 700 °C. The brittle FeB phase was not observed in any of the implantation borided M2 steel blocks.

5.0 Future Work

The obvious next step in this work would be to achieve implantation borided layer thicknesses closer to those of conventional boriding techniques. In order to accomplish this it is recommended that effect of implantation current density be studied over the range 500 to 2000 $\mu A/cm^2$. The goal of the work would be to determine the maximum current density at which boron can be delivered at prescribed implantation temperatures and energies without producing layers that exhibit inferior wear resistance. It is anticipated that the most wear resistant layers will be continuous and will contain none of the FeB phase. Establishing such limits should lead to an understanding of the true production capabilities of the ion implantation boriding process.

With any new technology the ultimate goal is to make things better, faster, safer and cheaper. To attain this goal with the ion implantation boriding system a number of things should be considered. This system is currently run with a hot cathode filament which limits the running time of the system and makes continuous boriding production impossible. A redesign of the system, possibly as an RF source, should be considered if mass production is ever to be considered with this technology. The difficulty of running an RF source and still maintaining the high crucible temperatures needed to evaporate the boron at a maintainable rate is definitely a technological challenge.

A point of possible interest that could be studied is the reduction in wear rate for the iron disc implantation borided at 950 °C, as seen in Fig. 13, as compared to the 900 °C implantation boriding. The 950 °C disc is also the only iron sample to have

Fe_3B as seen with XRD. Based on the existence of iron-nitrogen martensite [70], the fact that 950 °C is above the ferrite-austenite transition temperature and the long cool down time compared to most heat treatments with low carbon steels it is thought that the Fe_3B might be a byproduct of iron-boron martensite, much the same way that Fe_3C is a product of annealed iron-carbon martensite. After a preliminary literature search no information on iron-boron martensite was found, but further investigation of this concept is considered potentially useful.

Ion implantation boriding studies of other materials such as titanium, zirconium, chromium, molybdenum, intermetallics (NiAl), and cemented carbides may be in order. This technology, not requiring explosive and toxic gases, could make the boriding of these materials much more attractive. The high hardness, resistance to oxidation and chemical attack, resistance to molten metal wetting and wear resistance of borides of these metals make them attractive for applications ranging from aerospace to cathodes in aluminum production. [15,26,27,35,47,71]

References:

1) F.F. Ling, "Position Paper on Tribology," Journal of Tribology, 106, (1984), 24 - 25.

2) Donald F. Hays, "Research in Mechanical System: Tribology," Journal of Tribology, 106, (1984), 14 - 23.

3) Boronizing, Alfred Graf von Matuschka, Heyden & Sons, Inc., Philadelphia, PA, 1980.

4) K.G. Budinski, "The wear resistance of diffusion treated surfaces," *Wear*, 162-163, (1993), 757 - 762.

5) H.J. Hunger, G. Trute, "Boronizing to Produce Wear-resistant Surface Layers," *Heat Treatment of Metals*, 2, 1994, 31 - 39.

6) Anil Kumar Sinha, "Boriding," 437 - 447 in ASM Handbook Volume 4 Heat Treating ASM International, Materials Park, OH, 1991.

7) A. Erdemir, C. Bindal, G.R. Fensk, *Applied Physics Letter*, 68, (1996), 1637.

8) A. Erdemir, G.R. Fensk, F.A. Nichols, R.A. Erck, D.E. Busch, "Self-lubricating Boric Acid Films for Tribological Applications, "Proceedings of the Japan International Tribology Conference, Nagoya, Japan, (1990), 1797 - 1802.

9) Keith Stewart, "Boronizing Reduces Wear in Ceramic Processing Equipment," *Cermaic Industry*, May 1996, pp. 36 - 40.

10) Keith Stewart, "Boronizing Protects Metals Against Wear," *Advanced Materials and Processes*, 151, 3, March 1997, 23 - 25.

11) P. Goeuriot, F. Thevenot, J.H. Driver, "Surface Treatment of Steels : Borodif, A New Boriding Process," *Thin Solid Films*, 78, (1981), 67 - 76.

12) M. Carbucicchio, G. Meazza, G. Palombarini, "Surface Structure of Boride Layers Grown on Fe-C-Ni Alloys," *Journal of Materials Science*, 17, (1982), 3123 - 3128.

13) A.J. Ninham, I.M. Hutchings, "On the Morphology of Thermochemically Produced Fe_2B/Fe Interfaces", *Journal of Vacuum Science and Technology*, A4, 6, Nov/Dec 1986, 2827 - 2831.

14) Walter Fichtl, "Boronizing and its Practical Applications," *Materials in Engineering*, 2, Dec. 1981, 276 - 286.

15) H.J. Hunger, G. Trute, "Successful Boronizing of Ni-based Alloy," *Materials Science Forum*, 163 - 165, (1994), 341 - 346.

16) R.H. Biddulph, "Boronizing for Erosion Resistance," *Thin Solid Films*, 45, (1977),341 - 347.

17) M. Carbucicchio, L. Bardani, G. Sambogna, "On the Early Stages of High Purity Iron Boriding with Crystalline Boron Powder," *Journal of Materials Science*, 15, (1980), 1483 - 1490.

18) P. Goeuriot, R. Fillit, F. Thevenot, J.H. Driver, H. Bruyas, "The Influence of Alloying Element Additions on the Boriding of Steels," *Materials Science and Engineering*, 55, (1982), 9 - 19.

19) M. Carbucicchio, E. Zecchi, G. Palombarini, G. Sambogna, "Phase Composition and Structure of Boride Layers Grown on Laboratory-Cast Low-Chromium Alloys," *Journal of Materials Science*, 18, (1983), 3355 - 3362.

20) G. Palombarini, M. Carbucicchio, "On the Morphology of Thermochemically Produced Fe_2B/Fe Interfaces," *Journal of Materials Science Letters*, 3, (1984), 791 - 794.

21) K.H. Habig, "Wear Protection of Steels by Boriding, Vanadizing, Nitriding, Carburising, and Hardening," *Materials in Engineering*, 2, Dec. 1980, 83 - 92.

22) A.J. Ninham, I.M. Hutchings, "Solid Particle Erosion of Boronized Steels," 121 - 127, in Wear of Materials 1989, ed K.C. Ludema, ASME.

23) Nikola Rashkov, "Boronization of Steel Details in Electrothermal Rotary Layer," 25, in Proceedings of the 18th International Conference on Heat Treatment of Materials, 6 - 8 May 1980, Detroit, MI, American Society for Metals.

24) M. Carbucicchio, G. Palombarini, "Redistribution of alloying elements in 1100°C borided iron alloys," pp. 3.44, in Proceedings of the 3rd International Congress on Heat Treatment of Materials, ed. Professor T. Bell, 7 - 11 November, 1983, Shanghai, China.

25) S.C. Singhal, "A Hard Diffusion Boride Coating for Ferrous Materials," *Thin Solid Films*, 45, (1977), 321 - 329.

26) O. Knotek, E. Lugscheider, K. Leuschen, "Surface Layers on Cobalt Base Alloys by Boron Diffusion," *Thin Solid Films*, 45, (1977), 331 - 339.

27) G.V. Samsonov, A.P. Epik, "Boride Coatings," in Coatings of High-Temperature Materials, Henry H. Hausner ed., Plenum Press, NY, 1966.

28) G.V. Zemskov, N.G. Kaidash, "Boroaluminizing of Iron and Steel," in Diffusion Cladding of Metals, G.V. Samsonov ed., Consultants Bureau, New York, 1967.

29) L. Segers, A. Fontana, R. Winand, "Electrochemical Boriding of Iron in Molten Salts," *Electrochimica Acta*, 36, 1, (1991), 41 - 47.

30) Meng Qingen, Chen Zaizhi, "Boronization process in steel: theory of 'diffusion channel' model of boron atoms," pp. 3.8, in Proceedings of the 3rd International Congress on Heat Treatment of Materials, ed. Professor T. Bell, 7 - 11 November, 1983, Shanghai, China.

31) A. Ozsoy, Y.M. Yaman, "The effect of Thermocycling Liquid Boronizing on the Thickness of the Boride Layer," *Scripta Metallurgica et Materialia*, 29, 231 - 236, 1993.

32) Yan Pengxum, "Gaseous Boronizing with Solid Boron-Yielding Agents," *Thin Solid Films*, 214, (1992), 44 - 47.

33) Z. Zakhariev, R. Petrovo, "Gas phase reactions during simultaneous boronizing and aluminizing of steels," *Journal of Alloys and Compounds*, 196, (1993), 59 - 62.

34) L. Vandenbulcke, "Boron Deposition from the Reduction of Boron Trichloride Downstream from a Hydrogen Discharge," Proceedings of the International Ion Engineering Conference, 921 - 925, ed. Toshinori Takagi, 12 - 16 September 1983, Kyoto, Japan.

35) Steve Long, G.E. McGiure, "The Boriding of Chromium Photomasks for the Increased Abrasion Resistance," *Thin Solid Films*, 64, (1979), 433 - 438.

36) Yu V. Grdina, L.T. Gordeeva, "Diffusion Saturation of Steel from a Gaseous Medium by High Frequency Induction Heating," 53, in Diffusion Cladding of Metals, G.V. Samsonov ed., Consultants Bureau, New York, 1967.

37) T. Wierchon, J. Bogacki, T Karpinski, "Ion Boriding from the View-point of the Applied Gaseous Medium," 13, in Proceedings of the 18th International Conference on Heat Treatment of Materials, 6 - 8 May 1980, Detroit, MI, American Society for Metals.

38) Fay E. Gifford, "Plasma Silicon Nitriding and Iron Boriding," *Journal of Vacuum Science and Technology*, 10, 1, Jan/Feb 1973, 85 - 88.

39) P. Bielinski, K. Sikorski, T. Wierzchon, "Effect of glow discharge boriding on the distribution of elements within nickel stellite layers and the properties of these layers," *Journal of Materials Science Letters*, 15, (1996), 1335 - 36.

40) Fumiyoshi Miyashita, Katsuhiro Yokota, "Plasma-assisted low temperature boridation of pure iron and steels," *Surface and Coatings Technology*, 84, (1996), 334 - 337.

41) S. Saritas, R.P.M. Procter, V. Ashworth, W.A. Grant, "The Effect of Ion Implantation on the Friction and Wear Behaviour of a Phosphor Bronze," *Wear*, 82, (1982), 233 - 255.

42) Peter B. Madakson, "Friction, Wear and the Hardness of Boron-implanted 18W-4Cr-1V Steel," *Materials Science and Engineering*, 69, (1985), 167 - 172.

43) H.J. Kim, W.B. Carter, R.F. Hochman, E.I. Meletis, "Corrosion Behavior of Surface Films on Boron-implanted High Purity Iron and Stainless Steels," *Materials Science and Engineering*, 69, (1985), 297 - 301.

44) G.R. Rao, E.H. Lee, B.A. Chin, L.K. Mansur, "Effects of Simultaneous Boron and Nitrogen Implantation on Microhardness and Fatigue Properties of Fe-13Cr-15Ni Alloys," *Metallurgical and Materials Transactions A*, A25, Jan 1994, 193 - 202.

45) J.C. Pivin, P. Zheng, M.O. Ruault, "Transmission Electron Microscopy Investigation of the Structural Transformations in Titanium or TiAl Implanted with Nitrogen, Carbon, Oxygen, and Boron," *Material Science and Engineering*, A115, (1989), 83 - 88.

46) S. Raud, H. Garem, A. Naudon, J.P. Villain, P. Moine, "Wear Resistance Improvement and Structural Modifications of Boron Implanted Austenitic Stainless Steel," *Materials Science and Engineering*, A115, (1989), 245 - 251.

47) Emile J. Knystautas, Amarjit Singh, Michel Fiset, "Hardening of Ti-coated 4145 Steel Following Boron Ion Implantation," *Nuclear Instruments and Methods in Physics Research*, B19/20, (1987), 213 - 215.

48) O Henriksen, E. Johnson, A. Johansen, L. Sarholt-Kristensen, J.V. Wood, " The effect of Boron Implantation on the Corrosion Behaviour, Microhardness and Contact Resistance of Copper and Silver Surfaces," N*uclear Instruments and Methods in Physics Research*, B19/20, (1987), 247 - 252.

49) A.K. Suri, R. Nimmagadda, R.F. Bunshah, "Influence of Ion Implantation and Overlay Coatings on Various Physico-mechanical and Wear Properties of Stainless Steel, Titanium and Aluminum," *Thin Solid Films*, 64, (1979), 191 - 203.

50) Jun Saski, Masaya Iwaki, Wako Riken, "Friction Characteristics of B- and N_2-Implanted Fe-Cr Alloys," 421, in Processing and Characterization of Materials

Using Ion Beams, eds. Lynn Rehn, Joe Greene, Fred Smidt, Nov 28 - Dec 2, 1988, Boston, MA, Materials Research Society Symposium Proceedings Vol. 128.

51) G.S. Sandhu, M.L. Swanson, W.K. Chu, "Ion Implantation of Boron in Diamond," 707, in Processing and Characterization of Materials Using Ion Beams, eds. Lynn Rehn, Joe Greene, Fred Smidt, Nov 28 - Dec 2, 1988, Boston, MA, Materials Research Society Symposium Proceedings Vol. 128.

52) R.F. Hochman, H. Hong, K.Y. Kim, "A Study of Boron Implanted Stainless Steels," 123 - 125, in Proceedings of the Conference on Ion Implantation and Plasma Assisted Processes for Industrial Applications, eds. Robert F. Hochman, Hillary Solnick-Legg, Keith O. Legg, 22 - 25 May 1988, Altanta, Georgia, ASM International.

53) N. Millard, G. Marest, N. Moncoffre, J. Tousset, "Boron implantation into AISI 52100 steel," *Surface and Coatings Technology*, 51, (1992), 446 - 450.

54) Paul J. Wilbur, Ronghua Wei, "High-current-density metal-ion implantation," *Review of Scientific Instruments*, 63, 4, April 1992, 2491 - 3.

55) J.R. Conrad, "Plasma source ion implantation: A new approach to ion beam modification of materials," *Materials Science and Engineering*, A116, (1989), 197 - 203.

56) Shu Qin, Chung Chan, Nicol E. McGruer, "Energy distribution of boron ions during plasma immersion ion implantation," *Plasma Source Science and Technology*, 1, (1992), 1 - 6.

57) Jaroslav Kucera, Karel Stransky, "Diffusion in Iron, Iron Solid Solutions and Steels," *Materials Science and Engineering*, 52, (1982), 1 - 38.

58) C.M. Brakman, A.W.J. Gommers, E.J. Mittemeijer, "Boriding of Fe and Fe-C, Fe-Cr and Fe-Ni alloys; boride layer growth kinetics," *Journal of Materials Research*, 4, 6, Nov/Dec 1989, 1354 - 1370.

59) H. Kunst, O. Scaaber, *Hart.-Tech. Mitt.*, 22, 1, Translations HB 7122-I and HB 7122-II, 1967, 1 - 15.

60) ASM Specialty Handbook - Tool Materials, ed. J.R. Davis, ASM International, Materials Park, OH, 1995.

61) R. Wei, P.J. Wilbur, W.S. Sampath, D.L. Williamson, Y. Qu, L. Wang, "Tribological Studies of Ion-Implanted Steel Constituents using an Oscillating Pin-on-Disk Wear Tester," *Journal of Tribology*, 112, (1990), 27 - 36.

62) Annual Book of ASTM Standards, Designation G77-83, v. 03.02, ASTM, Philadelphia, PA, 1983, 453.

63) J.F. Ziegler, J.P. Biersack and U. Littmark, *The Stopping and Range of Ions in Solids*, Vol. 1, Pergamon, New York, 1985

64) R. Wei, J.J. Vajo, J.N. Matossian, P.J. Wilbur, J.A. Davis, D.L. Williamson, G.A. Collins, "A Comparative Study of Beam Ion Implantation, Plasma Ion Implantation, and Nitriding of AISI 304 Stainless Steel," *Surface and Coatings Technology*, 83, (1996), 235 - 242.

65) P.J. Wilbur, J.A. Davis, D.L. Williamson, J.J. Vajo, R. Wei, "High-Current-Density Broad-Beam Boron Ion Implantation," in press, *Surface and Coatings Technology*.

66) Dr. Don Williamson, Professor, Department of Physics, Colorado School on Mines, Golden, CO, personal communication.

67) John J. Vajo, Hughes Research Corporation, Malibu, CA, personal communication.

68) Bernd Rauchenbach, "Phase Formation in Iron After High-Fluence Ion Implantation," *Nuclear Instruments and Methods in Physics Research*, B80/81, (1993), 303 - 308.

69) Robert Frost, T.W. Pearson Ltd., Sheffield, England, personal communication.

70) K.H. Jack, "The Iron-Nitrogen System: The Preparation and The Crystal Structures of Nitrogen-Austenite (γ) and Nitrogen-Martensite (α')," *Proceedings of the Royal Society A*, 208, 1951, 200 - 215.

71) Matiur Rahma, Ching C. Wang, Weihua Chen, Sheikh A. Akabar, Cathleen Mroz, "Electrical Resistivity of Titanium Diboride and Zirconium Diboride," *Journal of the American Ceramic Society*, 78, 5, May 1995, 1380 - 82.